Submitted to Archiv für
Entwicklungsmechanik der Organismen,
Wilhelm Roux'

UCRL-19285
Preprint

cy 2

RECEIVED
LAWRENCE
RADIATION LABORATORY
OCT 8 1969
LIBRARY AND
DOCUMENTS SECTION

CELL LINEAGE IN THE DORSAL MESOTHORACIC DISC OF DROSOPHILA

Collin Murphy and Chiyoko Tokunaga
with the collaboration of William D. Hogan

August 1969

AEC Contract No. W-7405-eng-48

TWO-WEEK LOAN COPY

This is a Library Circulating Copy which may be borrowed for two weeks. For a personal retention copy, call Tech. Info. Division, Ext. 5545

LAWRENCE RADIATION LABORATORY
UNIVERSITY of CALIFORNIA BERKELEY

cy 2

UCRL-19285

DISCLAIMER

This document was prepared as an account of work sponsored by the United States Government. While this document is believed to contain correct information, neither the United States Government nor any agency thereof, nor the Regents of the University of California, nor any of their employees, makes any warranty, express or implied, or assumes any legal responsibility for the accuracy, completeness, or usefulness of any information, apparatus, product, or process disclosed, or represents that its use would not infringe privately owned rights. Reference herein to any specific commercial product, process, or service by its trade name, trademark, manufacturer, or otherwise, does not necessarily constitute or imply its endorsement, recommendation, or favoring by the United States Government or any agency thereof, or the Regents of the University of California. The views and opinions of authors expressed herein do not necessarily state or reflect those of the United States Government or any agency thereof or the Regents of the University of California.

CELL LINEAGE IN THE DORSAL MESOTHORACIC DISC OF DROSOPHILA*

Collin Murphy and Chiyoko Tokunaga
with the collaboration of William D. Hogan

Department of Zoology and Lawrence Radiation Laboratory
University of California, Berkeley

August 1969

*The authors wish to thank Professor Curt Stern for his encouragement and criticism of the manuscript and for his generosity in providing the gynandromorph data, Professor Chin Long Chiang for statistical advice, Mrs. Françoise Bacher and Mrs. Cole Ulrichs for technical assistance, and Mrs. Emily Reid for assistance in preparation of the figures. The unpublished English translation of the Noujdin paper was prepared through the courtesy of the National Science Foundation. This work was carried out under the auspices of the United States Atomic Energy Commission and supported in part by National Science Foundation Grant GB 6579.

Summary

1. Cell lineage in the dorsal mesothoracic disc of *Drosophila melanogaster* was studied by using mosaics for bristle color and bristle shape, resulting from somatic crossing-over induced by X-rays at 17–60 hours following egg deposition, as well as by using gynandromorphs, in which genetic marking occurs during early cleavage divisions. Data from spontaneously occurring mosaics studied by Sturtevant (1929) and Noujdin (1936) were re-evaluated.

2. Lineage relationships among the 11 mesonotal macrochaetae were traced by comparing ϕ correlation data from samples marked at different stages. Correlation diagrams lead to groupings of related macrochaetae, suggesting that related cells remain together (in accordance with the conclusion of Noujdin) and that there is a gradual restriction of cell lineage pathways during development. On a logarithmic scale, ϕ coefficients between pairs of macrochaetae are inversely proportional to the distance between them (in agreement with the suggestion by Sturtevant).

3. A more detailed, sectional analysis of most surface areas of the dorsal mesothorax was carried out by using mosaics on *hairy* flies on which microchaetae are present in normally naked areas. These mosaics were due to somatic crossing-over induced during the first larval instar. Analysis of the sample confirmed the results obtained by using macrochaetae alone. The frequency of occurrence of marked bristles varies in different disc regions, which suggests a gradient pattern of cell division rate within the disc. Distance between bristles or

sections does play a role in their genetic relationship to each other. However, in some sections found to be intimately related by cell lineage, the role of distance is secondary (particularly in parts of the disc which may have differential directions and rates of growth).

Application of principal-component analysis to the sectional data gives a relatively unambiguous method for separating the sections into six clusters. With one exception, the clusters so defined are groups of contiguous sections.

Each section studied was found to be significantly correlated with its surrounding and neighboring sections; most marked patches on individual specimens are also contiguous. "Passive migration" of groups of cells can be invoked as a developmental process in a few special cases. In general, cell lineage is nonrandom, in that the spatial relationship among cells developing from the same line is preserved throughout ontogeny.

Introduction

Cell lineage studies in Drosophila were originated by Sturtevant (1929). In his method of investigation, "mosaic" individuals with patches of phenotypically distinguishable tissue are produced by genetic techniques. The cells of a "marked" patch in these adult specimens are assumed to be related by descent from a common ancestral cell in which the genetic change occurred. With two exceptions, Sturtevant's pioneering study suggested the following basic concept of Drosophila development: that specific, determined regions of the adult body surface arise

from particular imaginal discs. Other workers (Birmingham, 1942, and Stern, 1963) later found that the two exceptional body areas described by Sturtevant (cephalic and sternopleural regions) also arise from specific imaginal primordia. The validity of Sturtevant's interpretation has been demonstrated repeatedly in other investigations: e.g., Noujdin (1936), Stern (1940), Bodenstein (1941), Gehring (1966), and Murphy (1967).

In line with the mode of development described by Sturtevant, each dorsal mesothoracic or "wing" disc gives rise to one wing and exactly one-half of the mesonotum (dorsal mesothorax) with its eleven constantly positioned macrochaetae and numerous microchaetae, as well as to the meso-, ptero-, and postpleurae. However, in contrast to the fixed developmental fate of the wing disc as a whole, specifically with regard to the mesonotal primordium within the disc, Sturtevant concluded that cell lineage was indeterminate. Analyzing a sample of 112 mosaics affecting the right or left halves of the mesonotum, he found that lineage relationships could not be traced for any pair of the 11 macrochaetae. Marked patches seemed to have been produced in random fashion, varying in size and shape. In addition, the calculated probability (as indicated by Yule's Coefficient of Association) that any particular pair of macrochaetae would be affected in the same half-mesonotum appeared to be only a function of the distance between them, independent of the direction of the line joining them. These calculations were carried out only for the macrochaetae.

On the basis of a larger sample of mosaics, and including areas marked by microchaetae as well as macrochaetae in his calculations,

Noujdin (1936)[1] reached somewhat different conclusions. He scored for occurrence of marked patches over the entire half-mesonotum by arbitrarily dividing it into a number of sections approximately equal in size. From the incidence of marked spots, he calculated the "Bravais" or ϕ correlation coefficients between individual sections, later grouping highly correlated sections into larger "regions." In contrast to the view of Sturtevant, Noujdin's interpretation indicated a lack of dependence between the magnitude of correlation and the distance between the sections. Moreover, he found that direction was important, in that correlations between pairs of sections were higher in the anterior-posterior direction than laterally. Noujdin suggested that cell lineage of the mesonotum was nonrandom in that (1) all cells within the "regions" composed of highly correlated sections were lineally related and that (2) the different "regions" develop from primordia with separate cell lineages.

The mosaics studied by Sturtevant arose in Minute-n stocks, presumably by somatic crossing-over (see Stern, 1936), whereas the sample obtained by Noujdin resulted from position-effect variegation in flies having scute-8 inversions. Both types of mosaicism are clonal and are suitable for comparison, at least in the eye (Becker, 1966; Baker, 1967). However, both sets of data are heterogenous in that they may include patches arising at various times in development. The conflicting conclusions of the two authors may be due to their different methods of analysis, different natures of their samples, or both. The availability of more uniform samples, namely mosaics arising from somatic crossing-over induced by X-rays during limited periods of development, has led us to re-examine the question of cell lineage within the mesonotum.

Materials and Methods

Sturtevant and Noujdin employed two different methods of recording their data. Scoring of mutant patches by means of the macrochaetae alone, as in Sturtevant's analysis, is advantageous with respect to uniformity of the sample unit of the 11 macrochaetae, although extensive areas of the mesonotum which contain no macrochaetae are automatically eliminated from study. Arbitrary division of the mesonotum into sections by Noujdin's method succeeds in including all surface areas but scoring is complicated by heterogeneity of markers; i.e., some of his sections contain only macrochaetae or microchaetae or no chaetae. Moreover, Noujdin describes borderline cases in which assignment of a patch to one section or another was uncertain.

The first part of our investigation consisted of a comparison of macrochaetal data from X-ray-induced mosaics with results of the previous investigators. One group of mosaics was produced by X-ray induction of somatic crossing-over in the second chromosome as described by Tokunaga and Arnheim (1966). Larvae were irradiated[2] at times ranging from 17 to 60 hours after egg deposition (total dose 1000–1500 r). These authors obtained flies having patches of yellow (1–0.0), not-Bristle (2–58.0) or yellow, Bristle tissue on not-yellow, Bristle background; 494 male half-mesonota with marked patches involving macrochaetae were collected from their material. Out of the total of 494 half-mesonota, 6.3% of the mosaics were obtained from irradiation at 17–22 hours, 28.6% at 22–32 hours, 16.1% at 33–43 hours, 27.6% at 45–50 hours, and 21.4% at 50–60 hours. All of these were "mixed" half-mesonota, i.e., having tissue of more than one phenotype. The size and shape of each marked

spot were recorded on standardized maps of the mesonotum (after Plunkett, 1926; see Fig. 1). These samples were subjected to analysis of spots by using only the macrochaetal scoring method.

For another comparison of macrochaetae, we studied drawings of male tissue spots from 325 "mixed" half-mesonota of gynandromorphs which C. Stern had examined and scored on Plunkett's diagram. Genotypes were as follows: the majority were y ac sn^3 (yellow, achaete, $singed^3$)/R(1) 2 (Ring-X-chromosome #2) females with spots of y ac sn^3 male tissue; a few were y w (yellow, white)/R(1) 2 females with y w male spots; a few others were sn^3/R(1) 2 females with sn^3 male patches. (Loci: white, 1–1.5; achaete, 1–0.0; $singed^3$, 1–21.0).

The second part of our investigation was designed to include marked patches involving microchaetae, to cover areas of the mesonotum and mesothorax not studied previously, and eventually to facilitate comparison with the results of Noujdin. Flies were homozygous for hairy (h, 3–26.5), having microchaetae present on normally naked regions, including the dorsal and ventral surfaces of the scutellum, several additional areas of the mesonotum, on the mesopleura, and occasionally on a triangle of tissue lying medially between the pteropleura and inferior postpleura (see Fig. 2, Section #62).

To produce mosaics, larvae of the genetic constitution y/+; h/h were irradiated[2] at 24–48 hours following egg deposition (total dose, 1500 r). Somatic crossing-over between yellow and the kinetochore resulted in patches of yellow (y/y) tissue on not-yellow (+/y) background on hairy (h/h) flies; 502 such "mixed" mesonota were collected. The mesonotal and pleural regions were arbitrarily

divided into 62 separate sections; the 11 macrochaetae comprised additional sections (actually points) 63–73 (Fig. 2). Outlines of the patches were first drawn on Plunkett's diagram (without sectional divisions). The sectional outline map was superimposed on an individual drawing by viewing both through a transparency illuminator; each of the sections was then scored as to presence or absence of yellow chaetae.

It must be noted that in seven of the sections (21, 40, 48, 51, 53, 54, and 62) there are very often no microchaetae present even in hairy flies. Therefore, statistical comparisons were generally limited to the remaining 66 sections, which have a much more even distribution of microchaetae.

The following statistical methods were used for analysis of the data:

1. Calculation of ϕ

Among the 11 macrochaetae, correlations between the 55 possible pairs of bristles were calculated by use of homogeneity χ^2 tests and converting to ϕ coefficients. For example, taking the first pair of bristles in the 17–60-hour X-ray series appearing in Table 1, one finds

	Cases Anp marked	Cases Anp not marked	Total
Cases Pr marked	26 (observed) 6.2 (expected)	45 (observed) 64.8 (expected)	71
Cases Pr not marked	17 (observed) 36.8 (expected)	406 (observed) 386.2 (expected)	423
Total	43	451	494

$\chi^2 = 80.9$ $p = < 0.0005$

χ^2/total no. specimens $= 80.9/494 = \phi^2$, $\phi = +0.41$

ϕ = ϕ coefficient, Pearson's mean-square contingency, or Bravais' correlation coefficient; ϕ is itself a derivative of the point-biserial correlation coefficient, r.

Range: +1 to -1; ϕ is positive when observed > expected in the "both marked" cell in the table.

The calculation is equivalent to that employed by Noujdin in the analysis of his own data and in his recalculation of the results of Sturtevant, although he did not compute χ^2 or probability values. The ϕ coefficient is statistically preferable to Yule's Coefficient of Association, at least according to Noujdin, who quotes Chuporoff (1922) and Diakonoff (1922) (exact references to these papers are not given) to the effect that the Yule's Coefficient gives a raised correlation.

2. Calculation of the Point-Biserial r

In our study of the 73 artificial sections (including the macrochaetal "points") of the mesothorax in the second series of experiments, the point-biserial correlation coefficients (r_{pbi}) were calculated for all pairs of sections (a computer was utilized). For example, the correlation between sections 1 and 2 was calculated as follows:

	Cases #1 marked	Cases #1 not marked	Total
Cases #2 marked	36	13	49
Cases #2 not marked	17	436	453
Totals	53	449	502

$$r_{pbi} = \frac{(Mp-Mq)\sqrt{pq}}{\sqrt{p'q'}},$$

where $Mp = 36/49 = 0.735$ $\quad p' = 53/502 = 0.106$

$- Mq = 17/453 = \underline{0.038}$ $\quad q' = 449/502 = 0.894$

0.697

$p = 49/502 = 0.098$

$q = 453/502 = 0.902$

and $pq = 0.0084$ $\quad p'q' = 0.0948$

$\sqrt{pq} = 0.297$ $\quad \sqrt{p'q'} = 0.307$

$$\underline{r_{pbi}} = \frac{(0.697)(0.297)}{0.307} = +0.674$$

3. Principal-Component Analysis[3]

By use of the hairy phenotype, most regions on the surface of the mesonotum and mesopleura could be analyzed in terms of their relationships to each other. The most direct approach to such a study is to examine relationships of individual artificial sections to all other sections, as in Noujdin's analysis, taking sections one at a time and comparing the results. By using a multivariate technique, however, relationships between all the sections can be studied simultaneously and groupings can be derived more accurately and efficiently. Principal-component analysis may be used to examine whether the artificial sections can be classified into groups, and provides a specific basis for such grouping as may be indicated.

If there were several lineages which developed into a coherent pattern (i.e., basically the same for every fly) on the mesothorax, then principal-component analysis would separate the lineages into appropriate groups of points in principal coordinate space. Thus our analysis attempts to treat the data from the 73 sections (including the 11 macrochaetal "points") so that if natural groupings existed, they would be made evident.

In the analysis, each specimen in our sample was regarded as an independent realization of a random vector. Each component of this random vector can be identified with a unique point in p-dimensional Euclidean space (Dempster, 1969); in this case, p = 73, corresponding to the 73 sections. The coordinates of each such point are dependent exclusively on the probability distribution of the random vector through the covariance matrix. Sample estimates of the coordinates were obtained by performing upon the sample covariance matrix the operations outlined.[4]

The application of this method to sample data involves finding the (p = 73) eigenvalues, and corresponding eigenvectors of the sample covariance matrix (a computer was utilized). The eigenvalues are rank-ordered in decreasing sequence, corresponding to the amount of variance they describe. Their corresponding eigenvectors are written columnwise in the same order. The rows of the resulting matrix of eigenvectors are the estimated coordinates of the sections.

The vector of principal components forms an orthogonal basis for a p-dimensional vector space, with covariance as inner product. Points in this space correspond to random variables which are linear combinations of the principal components; the length of a vector drawn from the origin to such a point is equal to the standard deviation of that random variable; the cosine of the angle between two such vectors is equal to the correlation between the two corresponding random variables. Hence, if a set of points in this space formed a compact cluster, then (1) they would have approximately the same standard deviation and (2) they would be intercorrelated, with a lower bound equal to the cosine of the smallest angle whose sides enclose all the points within the cluster.

Each artificial section corresponds to a point in the space of principal coordinates. Since the principal components are of different lengths, however, each coordinate of each section must be multiplied by the length of the corresponding principal component before the point is plotted. Because no mechanism for utilizing the higher dimensions was available, coordinates beyond the first three were ignored in defining clusters. The first three principal components represent 44% of the total marginal variance in the sample. Results of plotting the sections using the first two principal coordinates are given in Fig. 8 (e.g., for section 1, X and Y coordinates are +0.162 and -0.150).

The points were not labeled as to section number until after the cluster boundaries were decided upon. In this way, the clusters were determined in a "blindfold" manner, so that their boundaries were not prejudged. The clusters were then "decoded" and the sectional map was divided into corresponding segments (see Figs. 8 and 9a). The third principal coordinate (or Z coordinate) was utilized in deriving intracluster groupings, as plotted in Fig. 10, which were then transferred to the sectional map (Fig. 9c).

The foregoing calculation was repeated, omitting data from the seven sections sparsely covered with chaetae listed above. (This operation reduced the total number of half-mesonota to 498.) The only differences for the eigenvectors computed for the remaining 66 sections were at the third decimal place, i.e., coordinates were essentially identical, which justifies omission of the sections in terms of their contribution to the total variability.

Results

I. Frequency of Occurrence of Marked Bristles

Occurrence of marked patches involving the 11 macrochaetae on half-mesonota of specimens with X-ray-induced somatic crossing-over and in gynandromorphs is summarized in Table 1, according to simultaneous involvement of the 55 possible pairs of bristles. In Table 2, these specimens as well as Sturtevant's Minute-n series (1929) are compared with regard to frequency of involvment of individual bristles in marked spots. Similar data are not available from Noujdin's paper (1936).

The four samples taken as whole groups differ with respect to mean frequency of involvement of macrochaetae in a marked spot, as is shown by the F test for comparison of two means, summarized in Table 3. The two X-ray series do not differ significantly; all other comparisons reveal significant differences at the 5% level. Therefore, we can assume that the gynandromorph sample, having the highest frequency, has marked spots initiated at the earliest time, that there is a later induction in the Minute-n sample, and that the X-ray-induced mosaics, having the lowest frequency, are initiated still later in development.

The sizes of the marked patches found within different groups of specimens support the above assumption as to chronological order of induction. As shown in Table 4, the average patch size in gynandromorphs is very large, involving 6.6 of the 11 macrochaetae (4.4 if only "mixed" discs are considered), whereas in both X-ray-induced series, the average patch is much smaller, containing about 2.2 macrochaetae, indicating a later initiation of the marked cells. (There are no data for patch sizes except in the case of "singles" in the Minute-n series.)

Moreover, among the 502 specimens studied by the sectional method (24–48-hour X-ray-induced series) in the second part of our investigation, the average marked spot involves only 7.88 of the 73 sections and the most frequently occurring size involves only one section (Table 5), again indicating a late induction.

The above results from comparisons of average size of patches in each sample are further confirmed by analyzing each of the eleven macrochaetae. The frequency of involvement in marked patches among the different series is shown in Table 2. Considering only their face values, frequencies of involvement follow the same order as in Table 3 for seven of the 11 macrochaetae; that is, highest for gynanders, followed by the Minute-n, then the two X-ray series. Only the Psa, Ppa, Asc, and Psc do not conform exactly to this pattern. The Minute-n series is unique with respect to the very low frequencies of involvement of the scutellar bristles.

Considering the four sets of data in Table 2, significant differences at the 5% level (χ^2) between frequencies of occurrence for individual bristles exist in 35 of the 55 possible comparisons. The 20 pairs with insignificant differences are indicated by braces joining them. The 35 significant differences may be summarized as follows: The gynanders differ from the Minute-n specimens with respect to frequency of involvement of six of the macrochaetae, from the 24–48-hour X-ray series with respect to 10 macrochaetae and from all 11 macrochaetae of the 17–60-hour X-ray series. The Minute-n specimens differ from the 24–48-hour and 17–60-hour X-ray series in the cases of seven and

nine macrochaetae, respectively. Finally, the two X-ray series differ from each other with respect to only three of the 11 bristles.

In addition to the foregoing differences among the various series, χ^2 tests carried out within each experimental group indicate that, regardless of the origin of the sample, the different macrochaetae do not have the same frequencies of involvement in marked patches. For example, in the 17–60-hour X-ray series, the presutural bristle is affected in only 14% of the specimens, whereas the anterior dorsocentral is affected in 29%. These variations suggest a difference in susceptibility or in growth patterns, or both, among cells in different locations at the time of mosaic initiation; i.e., induction of marked cells may not occur at random in the mesonotal anlage.

When data from Table 2 are considered with reference to bristle position (see mesonotal map in Fig. 1) in the adult, frequencies are generally lower for anterior bristles such as the presutural and notopleural macrochaetae than for the posteriorly positioned postalars and scutellars. Moreover, frequency patterns are similar for the four sets of data (with the main exception being the low frequencies for scutellars in the Minute-n series), indicating general differences in sensitivity to mosaic induction or variable growth patterns in different parts of the disc.

The frequency differences indicated by study of macrochaetal reference points are revealed as part of a larger gradient pattern when other sections of the half-mesonotum are considered in the second part of our study (24–48-hour X-ray data, Fig. 3). There is an increase in frequency of marked bristles from anterior to posterior

around the lateral edge of the mesonotum, as noted for the macrochaetae. The anterior dorsocentral region is higher in frequency than the posterior dorsocentral region, and the region of highest occurrence is concentrated at the midline (sections 7 and 8), somewhat anterior to the level of the anterior dorsocentral. Frequencies decline gradually over the half-mesonotum in sections farther away from this peak.

The existence of the gradient pattern suggests that the higher parts of the gradient may be associated with higher rates of cell division. As discussed later, the largest "cluster" of sections grouped together by principal coordinates (Cluster II, Fig. 9a) includes the sections which are in the highest part of the gradient. From this we can conclude that the cell-division rate was higher in this area than in the lower parts of the gradient, at least after the initiation of mosaicism. The same reasoning may also apply to the situation at the time of initiation, since it is understandable that a higher rate of cell division would be associated with a greater probability of somatic crossing-over. (In this regard, Stern, 1936, noting significant differences in frequency among the tergites and between head, thorax, and abdomen, found that the incidence of somatic crossing-over was dependent on the spatial ontogenetic pattern.)

II. Correlation Studies and Cell Lineage

A. Correlations Between Pairs of Macrochaetae

Phi coefficients calculated from the material of Sturtevant and Noujdin as well as from gynandromorphs and X-ray-induced mosaics are presented in Table 6. In the 24–48-hour X-ray series, only those ϕ values which are positive and significant are indicated.

1. Correlation and distance

Sturtevant measured the distances between bristles on Plunkett's diagram, assigning them the units given in the second column in Table 6. From inspection of the distances and the corresponding Yule Association Coefficients, he concluded that "development is indeterminate, in that the genetic relationship of two trichogenic cells, is on the average, inversely proportional to their distance apart ···." Indeed, when a correlation diagram is constructed using the Minute-n data and Yule's coefficients, the strength of association, as indicated by the number of connecting lines, seems to increase as distance between macrochaetae decreases (Fig. 5d).

The essential correctness of Sturtevant's statement is further demonstrated when ϕ coefficients are plotted against distance on log-log paper. This operation was carried out for the first four sets of coefficients in Table 8, resulting in Figs. 4a–d, which may be described briefly as follows:

Fig. 4a: (Gynandromorphs). Coefficients have the widest range of values among the four sets of data in Fig. 4. (Possible range +1 to -1.) The coefficients are concentrated at the extremes (high + or - values), and 41 of the 55 values are significantly different from 0 (χ^2 $p < 0.01$). (Lines crossing the graphs indicate significance levels.)

Fig. 4b: (17–60-hour X-ray series). Coefficients are scattered more uniformly throughout the range of possible values; 30 of 55 are significant.

Fig. 4c: (Minute-n series). Coefficients also uniformly scattered throughout range; 14 of 55 significant.

Fig. 4d: (Position effect series). Thirteen of the 22 coefficents calculated by Noujdin are significant.

In Fig. 4e, point-biserial r values calculated for the 24–48-hour X-ray series are used. Calculations were based on all 502 specimens (185 had affected macrochaetae); 25 of the 55 values are significant.

The straight lines on the log-log plots which result for each of the samples indicate that the relationship between ϕ coefficients (and in the last case, point-biserial r coefficients) and distance between bristle sites is actually an exponential one. This finding may be explained by a consideration of patch sizes among groups of specimens: (1) The average size of a marked patch in X-ray-induced specimens and in gynandromorphs is large enough to cover more than one potential bristle site (see Table 4). This is especially likely to occur if the distance between chaetae is very small, as in the case of the Pr and Anp, separated by only 4 units on the Plunkett diagram. (2) Conversely, very few of the patches in mixed discs are large enough to cover macrochaetal sites located many units apart; e.g., the Pr and Pdc, separated by 15 units. Thus, an essentially linear relationship is biased at both extremes of the scale and tends toward an exponential curve.

2. Grouping of Macrochaetae by Correlation Coefficients

The finding of the general relationship between the correlation of bristle pairs and their distance apart is in agreement with the argument of Sturtevant. However, more detailed analysis of the data reveals some interesting patterns of correlation when ϕ coefficients are compared with reference to actual locations of macrochaetae on the mesonotum. Figures 5a–c and e are constructed so that the number of lines connecting the macrochaetae is approximately proportional to the

magnitude of the coefficients. Only positive and significant ϕ coefficients are utilized. The differences among these figures are clearly related to the time of origin of mosaicism in each of the experimental series.

In gynanders, in which cells become "marked" during early embryonic stages, before establishment of the imaginal discs, macrochaetae may be separated into two groups of highly correlated bristles (Fig. 5a). One group of five bristles contains the Pr, Anp, Pnp, Asa, and Psa; the other group is made up of the six remaining macrochaetae. Lower ϕ coefficients connect the two groups. The correlation diagram indicates that cells ancestral to the macrochaetae appear to be restricted into two main developmental groups which do not subsequently intermingle. Marked tissue arising by cell division after establishment of these clusters could include presumptive bristle cells (or their ancestors) within only one or the other of the restricted areas. Individual variations in cell lineage within the established disc, i.e., in the position of the hypothetical "constriction" between the regions, could account for the weaker correlations connecting the two main groups. It must be emphasized that the lineage relationships indicated in correlation diagrams can represent only average patterns of development. In individual specimens, marked patches often overlap the "regions" or fail to include the entire region. (For an illustration of specimens with overlapping regions, see Stern, 1940.)

In contrast to the gynandromorph data, the series in which somatic crossing-over was induced 17–60 hours following egg deposition

(in which the vast majority of individuals were in larval stages at the time of irradiation), the strongest correlations suggest separation of the macrochaetae into four smaller groups (Fig. 5b): (Group 1)--Pr, Anp; (Group 2)--Pnp, Asa, Psa; (Group 3)--Adc, Pdc, Apa, Ppa; (Group 4)--Asc, Psc. The earlier pattern of development as described for gynandromorphs may also be observed in this figure. There is a similar lack of strong connection between the Psa and the Apa and their respective related macrochaetae. Furthermore, weaker correlations connect X-ray groupings 1 and 2, which together are equivalent to gynandromorph Group 1. In addition, X-ray Groups 2 and 3 are joined by weak correlations corresponding to those between the two gynandromorph clusters.

The 17–60-hour X-ray data indicate a more restricted pattern of development superimposed upon our hypothetical original division into two main areas, as if each of the two large blocks of tissue segregates into two smaller blocks which subsequently develop as independent cell lines. Marker patches induced after this subdividing could involve only the presumptive macrochaetae included in a particular restricted region.

The early determination of the mesonotal anlage into two separate areas, as best revealed by the gynandromorph diagram, is also indicated by the large number (42 out of 55) of significant ϕ coefficients in that series (both positive and negative). The high numerical values of ϕ, either positive or negative, are expected if a presumptive macrochaeta early becomes included in one of only two possible lines of cell lineage. In later stages, as the two large areas became subdivided,

there would be more opportunities for variation in the cell lineage pathway leading to an individual bristle. The 17–60-hour X-ray data do have a lower number of significant ϕ coefficients (only 30 out of 55). [χ^2 $p = 0.02 > p > 0.01$ for 42/55 vs. 30/55.]

The hypothesis of gradual restriction of cell lineage pathways during development is best supported by a comparison of the correlation diagram derived from the 24–48-hour X-ray series with those of the gynandromorphs and 17–60-hour X-ray series. In the last experiment, the patch-producing event occurs later than in the gynandromorphs (which originate in early cleavage divisions) but earlier than the average time of induced somatic crossing-over in the 17–60-hour series. (See Materials and Methods.) As might be expected, the correlation diagram for the 24–48-hour series (Fig. 5c) is roughly intermediate to the other two configurations. The five anteriorly located macrochaetae are bound together in one correlation group just as in Group 1 of the gynandromorph data (Fig. 5a). Connections between the Pnp, Asa, and Psa are strong enough to suggest a subgroup comparable to Group 2 of the 17–60-hour X-ray series (Fig. 5b). The remaining six bristles form a group very much like Group 2 of the gynanders (Fig. 5a), although connections are not so strong.

The Minute-n correlation diagram (Fig. 5e) cannot easily be related to either of the previous figures. Macrochaetae may be separated into the following groups: (Group 1)--Pr, Anp, Pnp, Asa, Psa, Apa, Ppa (Group 2)--Adc, Pdc; (Group 3)--Asc, Psc. There are strong connections between the Psa and the postalar bristles, a relationship not indicated in the other two series. The other series reveal many connec-

tions between the dorsocentrals and other macrochaetae; in this case, there is only one such correlation, that between the Pdc and the Ppa.

If one assumes that Minute-n-induced somatic crossing-over occurs with equal frequency during all developmental stages, the average time of occurrence of the genetic event leading to mosaicism would be much later than in the gynanders, and clusters of marked cells would be correspondingly smaller. It is true that the isolation of the dorsocentral and scutellar bristles as Groups 2 and 3 respectively argues for a time of origin of mosaicism comparable to that found in the 17–60-hour X-ray series. However, Group 1, containing seven macrochaetae, is larger than either of the clusters in the gynandromorph diagram. Thus, the Minute-n series seems to be a special case.

To summarize, in addition to confirming a general relationship between correlation and distance, we were able to trace cell lineage relationships between groups of macrochaetae by comparing correlation data from samples in which marked spots were initiated at different developmental stages. The data from gynandromorphs and 17–60-hour and 24–48-hour X-ray series do not conflict with each other, but the Minute-n sample differs from the first three sets. (Since only 22 of 55 possible ϕ coefficients were calculated by Noujdin for the position effect series and his paper did not include raw data for involvement of pairs of macrochaetae, the resulting correlation diagram was incomplete and was omitted from consideration.)

B. Sectional Analysis of the Dorsal Mesonotum

Of the 63 sections on the dorsal mesonotum scored for occurrence of yellow chaetae in the 24–48-hour X-ray series, 59 provided

sufficient data for analysis. The remaining sections, namely sections 21, 40, 48, and 51, with fewer than 10 occurrences (mainly due to lack of marker chaetae), were omitted from study.

1. Correlation and Distance

The inverse and exponential nature of the relation between correlation and distance suggested by our study of macrochaetae is also supported by sectional analysis. Using section 2 as an example, approximate distance between sections as measured on the Plunkett diagram is plotted against the point-biserial correlation coefficients for the section on log-log paper (Fig. 6). By inspection, the linearity of the plot appears to be disturbed only by the circled points; i.e., sections 7 through 13, which show a higher correlation than expected simply according to distance from section 2. This discrepancy is indicative of the intimate nature of the cell lineage relationship existing between these seven sections on the median strip of tissue, as will be discussed later.

2. Correlation Between Pairs of Sections

Hypothetical cell lineage relationships can be derived, as in the Noujdin investigation, from laborious comparison of all the sectional correlation patterns followed by study of actual outlines of marked patches. The following are the results of preparing correlation diagrams for individual sections from our data.

Without exception, each of the 59 sections was significantly correlated ($\chi^2 p < 0.05$) not only with all sections bordering it but also with many other sections. A sample pattern of correlation is shown in Fig. 7a for section 1, which is on the scutellum. The highly correlated sec-

tions are clustered near to it and are also concentrated in a longitudinal strip along the median line which extends to the most anterior region of the mesonotum. Extremely similar patterns are obtained for each of the scutellar sections, which suggests a close relationship between them.

In other mesonotal regions, different patterns of correlation are obtained, depending on the location of the section. For example, section 27 (Fig. 7b), which surrounds the Pdc (section 70, scored separately), shows correlational relationships with the scutellum and with a large area of the surrounding mesonotal surface, whereas section 28 (Fig. 7c) surrounding the Pdc (Section 71), is unrelated to the scutellum. Section 52, at the extreme lateral, anterior end of the mesonotum (Fig. 7d), is not related either to the median strip of sections or to the scutellum.

Regardless of the particular pattern of correlation for individual section, related sections always form a continuous group or cluster. This clustering of correlated sections is to be expected if groups of lineally related cells stay together in the developing disc. There are three interesting exceptions to this rule: Section 11 (Fig. 7e) is correlated with only two posterior sections among the scutellar divisions, excluding anterior connecting sections. Section 13 (Fig. 7f) is correlated with a sheet of sections which fails to include section 37. The continuous sheet of sections correlated with section 52 fails to include section 43. These statistical exceptions will be discussed later in connection with actual specimens which have discontinuous marked patches on the mesonotum.

3. Results of Principal-Component Analysis

Principal-component analysis provides a somewhat different approach to the cell lineage problem. The results of plotting the 59 sections

of the mesonotum and seven other sections of the mesothorax in principal coordinates are given in Fig. 8. As expected from the study of macrochaetae alone, clusters of points can be constructed. Further subdivision of these primary clusters is made possible by using the third principal coordinate (Z axis); the latter was the basis for including section 57 in Cluster VI (dotted line). The six clusters, designated by Roman numerals, were transferred to the mesothoracic map as diagrammed in Fig. 9a. Clusters include sections as follows:

Dorsal mesonotum and scutellum

Cluster I: 1, 2, 3, 18, 19, 20, 22, 23, 24, 72 (Asc), 73 (Psc)--the dorsal scutellum.

Cluster II: 4, 5, 6, 7, 8, 9, 10, 11, 12, 13, 15, 16, 17, 25, 26, 27, 39, 68 (Apa), 69 (Ppa), 71 (Pdc)--median strip of tissue, including Pdc and postalar area.

Cluster III: 14, 29, 30, 38, 70 (Adc)--midregion around Adc.

Cluster IV: 31, 32, 33, 34, 43, 44, 45, 46, 47, 49, 50, 52, 63 (Pr), 64 (Anp), 65 (Pnp), 66 (Asa), 67 (Psa)--notopleural, supraalar, and presutural regions.

Cluster V: 28, 35, 36, 37, 41, 42--midregion containing no macrochaetae.

Other disc regions

Cluster VI: 55, 56, 57, 58, 59, 60, 61--ventral scutellum, "arch," and mesopleura.

The principal-component diagram of the overall surface of the mesonotum given in Fig. 9a, utilizing mosaics induced in the 24–48-hour X-ray series, generally corroborates the conclusions derived from our earlier study of macrochaetae alone, using correlation diagrams. The macrochaetae in Fig. 9a fall into groups comparable to those in Figs. 5a, b, and c. The basic separation of the five anteriormost bristles from the other six is confirmed and the scutellar subgrouping derived in Figs. 5b and c is again revealed. However, principal-component analysis places the dorsocentral macrochaetae into separate clusters, which was not shown by our previous method. (Stern, 1938, found that the Adc and Pdc combine with different nerve trunks, running in opposite directions, which may indicate separate development).

Of great interest is a comparison of the principal-component diagram with Noujdin's original division of the mesonotum into nine regions (as modified to fit our map in Fig. 9b). In general, they are alike. The separation of the scutellum as an independent region is identical to our finding. Our Cluster II, the median strip of tissue, resembles his Region (II).

The main differences are as follows: (1) Noujdin concluded that the section containing the Asa could be placed in either Region (VII) or (VIII). Our macrochaetal correlation diagrams clearly group this macrochaeta with the Psa and Pnp, or in his Region (VIII). (2) Our Cluster IV corresponds approximately to Noujdin's Regions (III), (VI), (VII), and (VIII) combined. Thus, his separation, at least with regard to the macrochaetae, is comparable to that derived in our 17–60-hour X-ray series. Furthermore, utilization of the 3rd principal coordinate (see Fig. 9c) in the 24–48-hour X-ray series does result in a very similar intracluster grouping such that the Pr

and Anp are in one subgroup, and the Pnp, Asa, and Psa are in another. (3) Noujdin also found that the section containing the Adc (his section 14) is of a mixed nature, explaining that "it develops from the rudiment of Region III in some cases and from the rudiment of Region IV in others." Since his section 14 contained both macrochaetae and microchaetae, we have studied it as two sections, namely 70 (Adc) and 28 (microchaetae). We see (Fig. 9a) that the Adc (section 70) belongs to Cluster III and section 28 to Cluster V. Thus, separate cell lines may actually exist within one of the sections arbitrarily drawn by Noujdin. (4) According to Noujdin, the half-mesonotum is itself divided into upper and lower halves (with the exception of his Region II), although not in a rigidly differentiated sense. The clusters established by our analysis, however, do not have smooth boundaries and cannot be separated by a simple horizontal dividing line. (5) Noujdin's Regions (II) and (IX) are approximately equivalent to our Cluster II. (6) The five mesonotal clusters derived from the 24-48-hour X-ray data are generally larger than Noujdin's nine mesonotal regions, which may indicate initiation of spots at an earlier stage in the X-ray-induced series.

Although there are other differences in details between the two independently derived diagrams, at least some of them may be due to the availability of marked areas in our hairy sample, in contrast to the lack of them in Noujdin's specimens. This may be especially true for areas where there are microchaetae in hairy, but not in wild-type flies. For example, hairy flies have many extra microchaetae in the postalar and posterior dorsocentral regions, areas where the two figures differ slightly. Of course, variation between the two figures may also have resulted simply from differences in statistical treatment of the data.

4. Continuity of Clusters

With the exception of Cluster III, all the clusters defined in Fig. 9a are continuous with respect to actual location of the sections on the thorax. (The only gaps are where there were insufficient data.) This result was expected, since we have seen that all sections are significantly (positively) correlated with their bordering and neighboring sections. Cluster VI will be discussed separately. In Cluster III, section 38 appears to be isolated from the other four sections. It is tempting to think that after the initiation of the areas II, III, and V as clusters, the later proliferation of Cluster II or V or both resulted in pushing and pinching the developing Cluster III into two parts. A similarly dynamic picture of cell lineage may have been revealed in the case of section 11 (Fig. 7e), where originally related areas may have become separated during development.

When actual, as opposed to statistically derived, patches are studied, even more developmental variability is revealed. As was pointed out by Noujdin, the marked spots often overlap the boundaries of the clusters, fail to include entire clusters, are irregular in outline, and may show discontinuities. For example, in the gynandromorphs, 37 of the 325 (11.4%) of the specimens possess two or more mesonotal patches separated by wild-type tissue. Of these, 22 specimens have one patch involving the region of Cluster II anterior to the Adc and a separate patch involving one or both scutellar macrochaetae. Of the 407 mesonotal specimens in the 24-48-hour X-ray series, 126 individuals (31%) have two or more distinct patches. In 75 of these specimens, the separate patch or patches consist of only a single bristle. There were 21 cases of separate patches simultaneously involving the anterior region of Cluster II and the

scutellum (Cluster I). The discontinuity within actual marked patches covering the median anterior microchaetae and scutellar regions in both experimental groups helps to explain the correlation diagram for section 11 (Fig. 7e).

In Minute-n - induced somatic crossing-over, however, Sturtevant states: "...the male tissue in every case forms a single definite clearly-marked patch, with no outlying spots and with no female tissue in the patch."[5] His finding of complete continuity may be related to the small sample studied.

The occurrence of two or more separate patches on a half-mesonotum may be explained in two ways: either they represent independently induced marked cells, or a single event, producing marked cells which become separated during development, as discussed earlier. Independent induction is more likely to occur when there are large numbers of cells available for treatment, as in the 24-48-hour X-ray series (31% with two or more patches), than in the case of the gynanders (11.4% with two or more patches), which usually result from X-chromosome loss in early cleavages. It is also possible that some of the gynanders with two patches result from secondary loss of the ring-X in later developmental stages. On the other hand, separation of marked cells originating from the same line may be particularly likely to occur during cell migration, as in the formation of the mesonotal surface from the monolayer of disc material during pupation. These alternatives cannot be distinguished when individual cases are considered.

It is clear from study of individual specimens that factors of randomness are superimposed upon a generally ordered process of cell

lineage. If, however, lineage relationships were completely random, we should expect a much greater degree of mixing of cell types, or a "salt and pepper" pattern in the mosaics.[6] Instead, with the specific exceptions noted above, observations of individual specimens do support the hypothesis that, in general, blocks of related cells remain together within the developing disc. Relationships of regions are better defined, and clustering is best revealed by means of multivariate statistical treatment.

C. Sectional Analysis of Other Mesothoracic Regions

Two new areas of the mesothorax not previously studied were sections 55 and 56, on the ventral surface of the scutellum (shown flat on map, Fig. 2). These sections are significantly correlated (point-biserial r) with each other but with none of the other sections. (Sections 53 and 54 contained only two and eight cases with marked chaetae, respectively, so were excluded from analysis.)

On the mesopleura, section 58 is correlated only with section 60; section 59 is related only to section 61. These correlations suggest independence of development of the mesopleural region, at least after the time of initiation of mosaicism. Although these correlations also suggest independence of sections 58 and 60 from 59 and 61, principal-component analysis leads to a different conclusion, as mentioned later. (Section 62, with only four cases, was excluded from analysis.)

The regions contained in Cluster VI in the principal-component diagram (Fig. 9a), although representing rather widely separated parts of the mesothorax (the undersurface of the scutellum plus the mesopleura and "arch"), are actually located in approximately the same

horizontal plane when viewed from the side (see Zalokar, 1947). Although at present there are insufficient microchaetal markers available for study of cell lineage of the tissue surfaces located between all the sections of Cluster VI, it is possible that the entire pleural surface and the ventral side of the scutellum form an independent cluster of related cells. It is certainly clear that the two regions studied are more closely related to each other than to the dorsal surface of the mesonotum.

Section 57, the thin band connecting the ventral scutellar and pleural regions ("arch"), is found to be related only to the dorsal, posterior surface of the mesonotum by point-biserial correlations (Fig. 7g). However, the results of principal-component analysis, utilizing the third principal coordinate indicate that it belongs to Cluster VI, which includes only the ventral scutellum and mesopleura. One possible explanation for this discrepancy is that a spurious statistical result occurred due to the small number of cases (22) involved.

D. Intracluster Relationship

Groupings of regions within the clusters themselves were constructed by using additional information derived from principal coordinates. Intracluster subregions based on the third principal coordinate are derived by circling of clusters (as in the initial two-dimensional analysis), as shown in Fig. 10, and transferring cluster designations to the mesothoracic map (Fig. 9c).

Clusters I and VI appear to be homogeneous. With regard to Cluster VI, the intracluster grouping found by using only point-biserial coefficients is not supported.

Cluster II can be divided into about four subgroups, some of which are not contiguous on the mesothoracic map. Sections 6, 7, and 13 are isolated from the other subgroups in this dimension. Sections 14 and 29 form the only subgroup in Cluster III; the remaining points are highly scattered. In Cluster IV, there are four contiguous subgroups which separate the included macrochaetae into two different regions.

Not all the subdivisions are necessarily meaningful in terms of developmental history, but independent support exists for at least the one in Cluster IV. As mentioned earlier, in the correlation diagram for the 17–60-hour X-ray series (Fig. 5b), the Pr and the Anp may be placed in a group separate from the Pnp, Asa, and Psa macrochaetae, which is in agreement with Noujdin's subdivision of the mesonotum. Data from Sidoroff (1935) utilizing position-effect specimens also confirm this separation.

The isolation of points corresponding to sections in the mid-region of the mesonotum, especially for Cluster III, may reflect variability in growth patterns in areas of the disc formed from a combination of several cell lines.

Discussion

The paired dorsal mesothoracic discs are the largest of the imaginal anlagen, each containing the primordia of several large surface areas of the adult fly; namely, mesonotum, meso-, ptero-, and postpleurae, and the wing. According to Auerbach (1936), these discs originate in the embryo and are visible in newly hatched larvae as

small, invaginated, one-layered sacs. During the second instar, each disc proper can be distinguished as a thickening of cells which make up the inner wall of the sac (the outer wall forms the thin peripodial membrane). The disc grows by cell division throughout the larval instars, the fusiform cells being stacked somewhat like coins, perpendicular to the long axis of the disc. At pupation, the imaginal hypoderm coming from the proximal portion of the disc spreads over the mesonotal region of the thorax, replacing larval epidermis and finally, about 8 hours following puparium formation, fusing with material from other discs in the dorsal region. (Bodenstein, 1950). Meanwhile, a more distal portion of the disc invaginates, growing outward as a large, two-layered sac-like structure which represents the future wing. The most distal region of the disc, called the marginal ridge by Auerbach, persists in its original location during wing invagination; its adult counterpart has not been described.

Our analysis, which specifically deals with only mesonotal and pleural anlagen, reveals that the spatial relationship among cells developing from the same ancestral line is generally clonal; i.e., cell lines tend to be preserved as clusters, at least from the time of their genetic "labeling" early in ontogeny until their manifestation as marked bristles in the adult fly. Thus, on the one hand, Noujdin's hypothesis of the regional nature of mesonotal cell lineage is supported. Accordingly, Sturtevant's conclusion that the "genetic relationship of two trichogenic cells . . . is not dependent on whether the line joining them is longitudinal or makes any given angle with the long axis of the fly" must be modified, since the existence of clusters (or restricted regions) makes

direction a crucial factor in the pattern of development. On the other hand, as maintained by Sturtevant, distance between bristles does play an important role in their genetic relationship to each other, as generally confirmed by logarithmic graphs in our analysis. The important exceptions to the logarithmic rule occur in areas which are much more intimately related by cell lineage than their map distances would indicate. This situation is understandable if one assumes high growth rates in these particular regions coupled with specific directions of growth as mentioned for Cluster II. It should be emphasized that the role of distance is particularly clear in mesonotal disc primordia, since we are dealing with cell lineage within a single-layered epithelial tissue.

New information, dealing with the development of the entire dorsal mesothoracic disc (although at a comparatively gross level), made available since the early contributions of Sturtevant and Noujdin, lends further pertinence to the study of cell lineage. By means of cutting out and transplanting specific parts of the mature dorsal mesothoracic disc into metamorphosing hosts, Hadorn and Buck (1962) were able to construct a map of prospective regions within the disc. This experiment demonstrated that specific areas within the disc are already determined in mature third instar larvae: the future mesonotum is located in the proximal portion, the prospective wing in the distal region of the disc. The positional map derived for prospective macrochaetae of the mesonotum is clearly related to actual locations of bristles in the adult (see their Fig. 3), as are specific regions of the wing portion. (Pleural regions could not be mapped due to lack of marker chaetae.)

It is of great interest that the cluster relationships which we

derived for macrochaetae by marking cells much earlier in development (24–48- or 17–60-hour X-ray series) are in general agreement with the scheme of Hadorn and Buck. Specifically, their map separates presumptive macrochaetae into three regions: one group contains the presutural and the notopleurals, the second includes dorsocentrals, postalars and supraalars, the third contains only scutellars. The only point of disagreement with our data is with regard to the supraalars, which we find to be more closely related to the presutural and notopleurals. It is likely that this discrepancy is the result of the method of cutting and transplanting the disc, which is relatively crude compared with using genetically marked discs in situ. This correspondence means that the cell lineage relationships detected by marking cells in the first instar are maintained throughout development; no major reorganization of cell groups, at least with respect to those detectable using mesonotal macrochaetae, takes place between the first instar and pupation.

Although the Hadorn and Buck study did not include the pleural regions, our analysis shows that Cluster VI, containing the ventral scutellum and mesopleura, has a significant negative correlation with the remaining five (mesonotal and dorsal scutellar) clusters. That the pleural regions of the mature disc may be more closely related to the wing than to the mesonotal anlage was suggested in extirpation experiments (Murphy, 1967). It is possible that the pleurae may originate from the most distal part of the disc, which is on the opposite side of the wing pouch from mesonotal primordia, being spatially (and ontogenetically) separated from the proximal mesonotal regions by the wing

blade primordium, and that during pupation, the pleural hypodermis migrates to the pleural surface of the thorax, covering it in a manner analogous to mesonotal tissue on the dorsal surface. Future developmental study including proper cell lineage studies utilizing markers in mesonotal, wing, and pleural areas is necessary in order to locate the pleural primordia within the imaginal disc.

The spatial stability of cell lines within the dorsal mesothoracic disc as revealed by both transplantation and genetic marking techniques, favors a hypothesis of prepatterning of larval disc cells with regard to regional characteristics, followed by their final determination and positioning during pupation. Since the clonal nature of ancestrally related cells is the predominant cell lineage characteristic of the adult mesonotum and mesopleura, individual cell migration cannot play a major role in normal development. (The small percentage of noncontiguous patches on individual specimens, some of which represent independent events, also argues against a hypothesis involving migration of individual cells in the formation of the dorsal mesothoracic and pleural regions.) This conclusion is most clearly confirmed by our study of macrochaetal reference points with relation to other, larger (multicellular) sections of the mesonotum. In all cases, individual macrochaetae are significantly correlated with their surrounding and neighboring sections (point-biserial coefficients). No macrochaetae form noncontiguous portions of clusters (by principal component analysis, Fig. 9a).

Thus the situation found in normal development is quite different from the individual, autonomous migration of single determined cells to their proper adult sites, as was found in <u>in vitro</u> studies with artificially

mixed cell populations (Ursprung and Hadorn, 1962; Garcia-Bellido, 1966). Indeed, the only evidence for migration arising from the present study is limited to so-called "passive migration" (Ursprung, 1966) of a group of cells by differential forces between cell clusters as they grow and later as they move into position on the mesothorax during pupation. Examples of this kind of migration may be found in our Cluster III, which has one noncontiguous section, and in the isolated sections within clusters derived by using the third loading coefficient in principal-component analysis. This type of "passive migration" in situ was first described for the development of a sex comb site in Drosophila by means of a cell lineage study (Tokunaga, 1962).

An interesting parallel to the Drosophila case is found in development of ectoderm in the newt (Burnside and Jacobson, 1968). Following gastrulation, cells marked with natural pigmentation spots were traced by time-lapse cinematography. During formation of the neural plate, cells persist in positional relationships with their neighbors; i.e., there is no free migration of individual cells, but rather movement as a continuous sheet. When (infrequently) mitoses occur, daughter cells remain together. Similar direct observations of cell movement have not been carried out in Drosophila.

Mitotic activity within the larval wing disc has not been studied in detail, but the gradient of mitotic rates we have suggested over different regions of the dorsal mesothoracic disc provides new information regarding this basic aspect of disc development. The greatest rate of cell proliferation occurs in the mesonotal disc region, giving rise to the most extensive area of the mesonotum, Cluster II (compare gradient

map, Fig. 3, with cluster map, Fig. 9a). In contrast, the lowest rates are found in the region of the mesonotum bordering the point of insertion of the wing, which is a comparatively narrow band of tissue in the adult.

(By direct observation, regional differences in mitotic rate within the pupal wing were found by Stumpf, 1956. She noted that mitosis proceeds in a wave, first peaking in the proximal part of the wing and gradually declining there as new peaks arise distally during the period of 15–22 hours after pupation. Williams (1968) found differences in frequency of marked patches occurring on the dorsal and ventral surfaces of the wing in gynandromorphs. This may also reflect unequal mitotic activity in different parts of the disc.)

Footnotes

[1]The authors utilized an unpublished English translation.

[2]Using 140 kV, 4 mA, 1.5 mm. Aluminum inherent filtration plus 0.75 mm aluminum external filtration.

[3]This part of the study was done in collaboration with William D. Hogan, who suggested use of the criterion of clustering in the space of principal components to partition the sections; he also performed the necessary programming and computations and authored relevant parts of the text.

[4]The statistical origin of the method of principal components is due to H. Hotelling. References to the work of Hotelling, as well as a comprehensive discussion of multivariate methods, may be found in C. R. Rao (1965), especially pp. 501-504; see also "References," pp. 510-513.

[5]Sturtevant (1929) thought his samples were gynandromorphs rather than mosaics resulting from somatic crossing-over (which was not known until later) (Stern, 1936).

[6]In the position-effect specimens studied by Noujdin, there was "a whole series of cases of the presence of separate non-mosaic cells within the limits of a clearly delimited mosaic spot." This apparent intermingling of cell types possibly reflects a temperature sensitivity of the position-effect phenomenon which occurs late in development (Becker, 1966).

References

- Auerbach, C.: The development of the legs, wings, and halteres in wild type and some mutant strains of Drosophila melanogaster. Trans. Royal Soc. Edinburgh 58, 787-815 (1936).
- Baker, W. K.: A clonal system of differential gene activity in Drosophila. Develop. Biol. 16, 1-17 (1967).
- Becker, H. J.: Genetic and variegation mosaics in the eye of Drosophila. In: Current Topics in Developmental Biology, vol. 1. New York: Academic Press 1966.
- Birmingham, L.: Boundaries of differentiation of cephalic imaginal discs in Drosophila. J. Exptl. Zool. 91, 345-363 (1942).
- Bodenstein, D.: Investigations on the problems of metamorphosis. VIII. Studies on leg determination in insects. J. Exptl. Zool. 87, 31-53 (1941).
- --- The postembryonic development of Drosophila. In: Biology of Drosophila, ed. M. Demerec, p. 275-367. New York: Hafner 1950.
- Burnside, M. B., and A. G. Jacobson: Analysis of morphogenetic movements in the neural plate of the newt, Taricha torosa. Develop. Biol. 18, 537-552 (1968).
- Dempster, A. P.: Elements of Continuous Multivariate Analysis. Reading, Mass.: Addison-Wesley 1969.
- Garcia-Bellido, A.: Pattern reconstruction by dissociated imaginal disc cells of Drosophila melanogaster. Develop. Biol. 14, 278-306 (1966).
- Gehring, W.: Übertragung und Änderung der Determinationsquali-

täten in Antennenscheiben-Kulturen von Drosophila melanogaster. J. Embryol. Exptl. Morphol. 15, 77-111 (1966).

- Hadorn, E., and D. Buck: Ueber Entwicklungsleistungen transplantierter Teilstücke von Flügel-Imaginalscheiben von Drosophila melanogaster. Rev. Suisse Zool. 69, 302-310 (1962).
- Murphy, C.: Determination of the dorsal mesothoracic disc in Drosophila. Develop. Biol. 15, 368-394 (1967).
- Noujdin, N. I.: Genetic analysis of certain problems of the physiology of development of Drosophila melanogaster. (In Russian). Biol. Zhur. Armenii 5, 571-624 (1936).
- Plunkett, C. R.: The interaction of genetic and environmental factors in development. J. Exptl. Zool. 46, 181-244 (1926).
- Rao, C. R.: Linear Statistical Inference and its Applications. New York: Wiley 1965.
- Sidoroff, B. N.: Yellow-mosaics in the scute-8 line of Drosophila melanogaster. (In Russian). Biol. Zhur. Armenii 3, 737-739 (1935).
- Stern, C.: Somatic crossing over and segregation in Drosophila melanogaster. Genetics 21, 625-730 (1936).
- --- The innervation of setae in Drosophila. Genetics 23, 172-173 (1938).
- --- The prospective significance of imaginal discs in Drosophila. J. Morphol. 67, 107-122 (1940).
- --- The cell lineage of the sternopleura in Drosophila melanogaster. Develop. Biol. 7, 365-378 (1963).

- Stumpf, H.: Die Richtungen der Teilungsspindeln auf dem Puppenflügel von Drosophila im Verlaufe der Mitosenperiode. Biologisches Zentral. 75, 17-26 (1956).
- Sturtevant, A. H.: The claret mutant type of Drosophila simulans: a study of chromosome elimination and of cell lineage. Z. wiss. Zool. 135, 323-356 (1929).
- Tokunaga, C.: Cell lineage and differentiation of the male foreleg of Drosophila melanogaster. Develop. Biol. 4, 489-516 (1962).
- ---, and N. Arnheim, Jr.: Age dependence of the locations of X-ray induced somatic crossing over in Drosophila. Genetics 54, 267-276 (1966).
- Ursprung, H.: The formation of patterns in development. In: Major Problems in Developmental Biology. p. 177-213. New York: Academic Press 1966.
- ---, and E. Hadorn: Weitere Untersuchungen über Musterbildung in Kombinaten aus teilweise dissoziierten Flügel-Imaginalscheiben von Drosophila melanogaster. Develop. Biol. 4, 40-66 (1962).
- Williams, G.: Wing mosaics in Drosophila melanogaster. Master's thesis, Dept. of Zoology, University of California, Berkeley (1968).
- Zalokar, M.: Anatomie du thorax de Drosophila melanogaster. Rev. Suisse Zool. 54, 17-53 (1947).

Table 1. Number of times stated pairs of macrochaetae are simultaneously involved in marked patches in three groups of specimens. The numbers in the first row below each bristle name represent total cases involving that particular bristle in each series, and in parentheses, the number of cases in which only one bristle is affected ("singles"). The number of "singles" in the 24–48-hour X-ray series was not calculated.

		X-ray(hours)	
	Gynanders	17–60	24–48
Presutural (Pr)			
	119 (4)	71 (18)	31
Anp	88	26	15
Pnp	91	21	12
Asa	90	25	10
Psa	62	15	7
Apa	41	9	2
Ppa	38	6	2
Adc	62	22	7
Pdc	33	12	2
Asc	27	6	2
Psc	27	6	3
Anterior notopleural (Anp)			
	98 (5)	43 (10)	27
Pnp	79	11	10
Asa	71	11	6
Psa	45	5	4
Apa	25	5	0
Ppa	20	4	0
Adc	42	10	3
Pdc	17	6	0
Asc	9	4	0
Psc	9	4	0
Posterior notopleural (Pnp)			
	115 (2)	46 (2)	26
Asa	101	39	17
Psa	69	27	12
Apa	46	6	5
Ppa	38	4	4
Adc	60	14	7
Pdc	34	8	2
Asc	26	2	2
Psc	26	2	2
Anterior supraalar (Asa)			
	136 (2)	95 (12)	27
Psa	96	60	20
Apa	73	20	4
Ppa	61	13	4
Adc	84	39	8
Pdc	53	22	3
Asc	50	5	2
Psc	51	5	2

		X-ray(hours)	
	Gynanders	17–60	24–48
Posterior supraalar (Psa)			
	111 (7)	95 (8)	45
Apa	72	30	11
Ppa	61	18	10
Adc	73	50	12
Pdc	52	28	8
Asc	46	7	3
Psc	47	6	3
Anterior postalar (Apa)			
	153 (4)	85 (14)	32
Ppa	130	52	19
Adc	102	40	6
Pdc	90	36	10
Asc	111	24	7
Psc	108	22	6
Posterior postalar (Ppa)			
	147 (2)	97 (13)	38
Adc	99	42	10
Pdc	97	46	23
Asc	119	36	13
Psc	116	34	13
Anterior dorsocentral (Adc)			
	149 (13)	143 (42)	42
Pdc	95	52	21
Asc	84	23	8
Psc	84	20	9
Posterior dorsocentral (Pdc)			
	123 (17)	87 (11)	49
Asc	85	24	16
Psc	83	24	17
Anterior scutellar (Asc)			
	151 (1)	162 (24)	42
Psc	145	132	40
Posterior scutellar (Psc)			
	149 (1)	153 (20)	46
Number half-mesonota			
Grand total	325	494	185

Table 2. Frequency with which individual macrochaetae are involved in marked patches in specimens of different origins. Braces indicate that the differences between pairs are insignificant; χ^2 $p < 0.05$. (s. c. o. = somatic crossing over.)

Homogeneity within sample, χ^2 p =	Total number of discs	pr	anp	pnp	asa	psa	apa	ppa	adc	pdc	asc	psc	$\bar{X}$
< 0.01	325 discs, gynanders	0.37	0.30	0.35	0.42	0.34	0.47	0.45	0.46	0.38	0.47	0.46	0.406 ±0.07
< 0.01	112 discs, Minute-n-induced s. c. o.	0.29	0.21	0.22	0.33	0.37	0.33	0.45	0.38	0.27	0.19	0.12	0.287 ±0.10
0.05 > p > 0.01	185 discs, X-ray-induced s. c. o. (24-48 hr)	0.17	0.15	0.14	0.15	0.24	0.17	0.21	0.23	0.27	0.23	0.25	0.201 ±0.05
< 0.01	494 discs, X-ray-induced s. c. o. (17-60 hr)	0.14	0.09	0.09	0.19	0.19	0.17	0.20	0.29	0.18	0.33	0.31	0.198 ±0.08

Table 3. F test for comparing two means applied to four groups of specimens; degrees of freedom = 1, 20. Means are mean frequencies with which macrochaetae are involved in marked patches.

Means		Gynanders	Minute-n	24–48-hr X-ray
Gynanders:	0.406 ± 0.07			
Minute-n:	0.287 ± 0.10	$p < 0.01$ $F = 19.96$		
24–48-hr X-ray:	0.201 ± 0.05	$p < 0.01$ $F = 79.5$	$0.05 > p > 0.01$ $F = 7.06$	
17–60-hr X-ray:	0.198 ± 0.08	$p < 0.01$ $F = 41.6$	$0.05 > p > 0.01$ $F = 5.4$	$p > 0.05$ $F = 0.00001$

Table 4. Sizes of marked patches and their frequencies in three groups of specimens.[a]

Number of macrochaetae in patch	Gynanders (%)	X-ray (hours) 17–60 (%)	X-ray (hours) 24–48 (%)
1	12	36	39
2	8	38	30
3	5	11	16
4	12	5	8
5	7	5	5
6	9	3	1
7	4	<1	0
8	6	<1	0
9	3	<1	0
10	2	<1	1
11[b]	32	<1	0
Average size of patch (all discs) (macrochaetae)	6.6	2.3	2.2
Average size of patch; "mixed" discs only (macrochaetae)	4.4	2.2	2.2

Table 5. Distribution by total number of marked sections per disc in the 24–48-hour X-ray series (502 discs). All larger numbers (>4) of marked sections have frequencies < 0.05. Average number of sections marked per disc = 7.88.

Number of marked sections	Frequency	Proportion
1	128	0.255
2	69	0.137
3	47	0.094
4	36	0.072

Table 6. Phi correlation coefficients for the 55 pairs of macrochaetae in five groups of specimens. In position-effect series, blank space indicates absence of data from Noujdin's paper. "Distance apart" is as measured on Plunkett's diagram.

	Distance apart	Gynanders	X-ray (hours) 17–60	X-ray (hours) 24–48	Minute-n	Position effect
Presutural (Pr)						
Anp	4	0.73[a]	0.41[a]	0.41[a]	0.58[a]	---
Pnp	6	0.65[a]	0.29[a]	0.30[a]	0.56[a]	---
Asa	5	0.52[a]	0.17[a]	---	0.39[a]	---
Psa	7	0.28[a]	0.02	---	0.22	---
Apa	12	-0.19[a]	-0.02	---	-0.08	---
Ppa	13	-0.21[a]	-0.12	---	-0.09	---
Adc	9	-0.09	-0.02	---	0.16	---
Pdc	12	-0.16[a]	0.01	---	-0.11	---
Asc	17	-0.36[a]	-0.21[a]	---	-0.11	---
Psc	23	-0.36[a]	-0.20[a]	---	-0.14	---
Anterior Notopleural (Anp)						
Pnp	5	0.62[a]	0.17[a]	0.25[a]	0.66[a]	0.53[a]
Asa	6	0.41[a]	0.05	---	0.37[a]	0.26[a]
Psa	9	0.16[a]	-0.06	---	0.23	0.49[a]
Apa	12	-0.29[a]	-0.05	---	-0.01	---
Ppa	15	-0.32[a]	-0.08	---	0.01	---
Adc	12	-0.04	-0.04	---	-0.04	0.09
Pdc	15	-0.28[a]	-0.03	---	-0.07	---
Asc	19	-0.50[a]	-0.15[a]	---	-0.08	---
Psc	25	-0.49[a]	-0.15[a]	---	-0.18	0.09
Posterior Notopleural (Pnp)						
Asa	4	0.69[a]	0.53[a]	0.56[a]	0.58[a]	0.58[a]
Psa	5	0.41[a]	0.32[a]	0.20[a]	0.48[a]	0.49[a]
Apa	8	-0.11	-0.04	---	-0.02	---
Ppa	11	-0.18[a]	-0.03	---	0.20	---
Adc	11	-0.09	0.01	---	0.11	-0.04
Pdc	12	-0.13	0.00	---	0.01	-0.06
Asc	15	-0.35[a]	-0.19[a]	---	0.01	-0.10
Psc	21	-0.35[a]	-0.19[a]	---	-0.12	-0.14
Anterior Supraalar (Asa)						
Psa	2	0.64[a]	0.54[a]	0.48[a]	0.64[a]	0.68[a]
Apa	7	-0.11	0.05	---	0.21	---
Ppa	9	-0.02	-0.07	---	0.21	---
Adc	7	0.28[a]	0.13[a]	---	0.05	0.21[a]
Pdc	9	0.01	-0.07	---	-0.24	---
Asc	13	-0.16[a]	-0.29[a]	---	-0.05	---
Psc	19	-0.14	-0.27[a]	---	-0.05	-0.004
Posterior Supraalar (Psa)						
Apa	4	0.25[a]	0.19[a]	---	0.43[a]	---
Ppa	6	0.143[a]	-0.01	---	0.43[a]	---
Adc	7	0.29[a]	0.26[a]	---	0.10	0.30[a]
Pdc	7	0.14	0.15[a]	---	0.08	---
Asc	10	-0.08	-0.27[a]	---	0.14	---
Psc	16	-0.05	-0.26[a]	---	-0.10	-0.15[a]
Anterior Postalar (Apa)						
Ppa	4	0.76[a]	0.48[a]	0.44[a]	0.72[a]	---
Adc	9	0.40[a]	0.18[a]	---	-0.01	---
Pdc	6	0.41[a]	0.30[a]	---	0.16	---
Asc	7	0.49[a]	-0.05	---	0.18	---
Psc	13	0.47[a]	-0.05	---	0.03	---
Posterior Postalar (Ppa)						
Adc	7	0.40[a]	0.16[a]	---	0.01	---
Pdc	3	0.52[a]	0.39[a]	0.40[a]	0.26[a]	---
Asc	4	0.63[a]	0.05	0.143[a]	0.12	---
Psc	10	0.61[a]	0.04	---	0.06	---
Anterior Dorsocentral (Adc)						
Pdc	5	0.49[a]	0.31[a]	0.30[a]	0.53[a]	0.65[a]
Asc	11	0.19[a]	-0.23[a]	---	0.01	0.07
Psc	16	0.20[a]	-0.23[a]	---	-0.01	0.15[a]
Posterior Dorsocentral (Pdc)						
Asc	7	0.36[a]	-0.05	0.15[a]	0.17	0.19[a]
Psc	12	0.34[a]	-0.03	---	0.03	0.19[a]
Anterior Scutellar (Asc)						
Psc	6	0.94[a]	0.76[a]	0.88[a]	0.46[a]	0.90[a]

Table 7. Inter-cluster point-biserial correlation coefficients

	II	III	IV	V	VI
I	0.508[a]	0.141	-0.069	0.000	-0.100[a]
II		0.614[a]	0.031	0.294	-0.245[a]
III			0.303[a]	0.678[a]	-0.230[a]
IV				0.526[a]	-0.222[a]
V					-0.259[a]

Footnotes to Tables

Footnotes to Table 4:

a. In the Minute-n series, 33% of patches are "singles," having only one macrochaeta in the patch; no information regarding other patch sizes is available.

b. Discs not "mixed" with regard to macrochaetal types; all marked.

Footnotes to Table 6

a. $p < 0.01$ (χ^2 homogeneity test) except in the 24–48-hour X-ray series, where $p < 0.001$. Only positive, significant values are listed for that series.

Footnote to Table 7

a. χ^2 homogeneity test $p < 0.025$.

Figure Legends

Fig. 1. Map of the dorsal mesonotum of Drosophila, after Plunkett (1926). Macrochaetae (circles) are numbered from 63–73. Abbreviations for bristle names indicated, where A, P = anterior, posterior. Dots represent microchaetae.

Fig. 2. Artificial sections of the dorsal mesothorax used in scoring marked bristles. The ventral scutellum, "arch," and pleural regions of the map are drawn as if they are in the same plane as the mesonotum. Bold stripes indicate regions not studied.

Fig. 3. Frequency of occurrence of marked bristles within the 63 artificial sections and with respect to the 11 macrochaetae in the 24–48-hour X-ray series. Calculations based on 502 half-mesothoraces. Sections 7 and 8 form the peak of the gradient. Bold stripes indicate regions not studied.

Fig. 4. Log-log plots of correlation coefficients vs distance between macrochaetal pairs as measured on the Plunkett diagram in five groups of specimens. Dots on the arrowhead sides of lines represent coefficients which are significantly different from zero. (χ^2 $p < 0.01$). In Figs. a-d, ϕ coefficients are used; in Fig. e, point-biserial $\underline{r}$ coefficients are used (significance level also based on χ^2 homogeneity test).

Fig. 5. Correlation diagrams for four groups of specimens, using only positive correlation coefficients (either significant ϕ coefficients or Yule's Coefficients of Association-no significance level known),

where the number of lines connecting a macrochaetal pair is approximately proportional to the magnitude of the coefficient. Braces enclose groups of highly correlated bristles. Fig. a: Gynandromorphs. Fig. b: 17–60-hour X-ray series. Fig. c: 24–48-hour X-ray series. Fig. d: Minute-n induced somatic crossing-over series; Yule's Coefficients. Fig. e: Same as in Fig. d, using ϕ coefficients.

Fig. 6. Log-log plot of point-biserial correlations between section 2 and other sections vs their respective distances from section 2 as measured on the map in Fig. 2. Only dorsal mesonotal sections are considered (24–48-hour X-ray series). By inspection, the circled points seem to disturb linearity of the plot. Points numbered by section.

Fig. 7. Positive, significant (χ^2 $p < 0.001$) correlations of representative sections with other sections. Correlated sections are shaded; sections with insufficient data for analysis are faintly stippled. Fig. a: Correlations with section 1. Fig. b: Correlations with section 27. Fig. c: Correlations with section 28. Fig. d: Correlations with section 52; note lack of correlation in section 43. Fig. e: Correlations with section 11; note lack of correlation in sections 2, 3, 18, 19. Fig. f: Correlations with section 13; note lack of correlation in section 37. Fig. g: Correlations with section 57.

Fig. 8. Visual grouping of numerically coded sections into clusters. The position of sectional points is determined by using the first

two principal-components as X and Y coordinates (see text). In section 57 (dotted line), inclusion in Cluster VI based on use of the third principal component or Z coordinate.

Fig. 9. a: Translation of the principal-component analysis clusters in in Fig. 8 onto the mesothoracic map. All clusters are contiguous except for Cluster III. Sections shown in white: insufficient data for analysis. Heavy stripes indicate regions not studies. Fig. b: The nine regions of the mesonotum derived from position-effect data by Noujdin (1936), as approximated on our map. The relationship of the Asa and Adc bristles (question marks) to the regions was doubtful, according to Noujdin. Fig. c: Translation of the intracluster groupings plotted in Fig. 10 onto the mesothoracic map. Heavy stripes indicate regions not studied. The question marks indicate sections not included in any of the subclusters.

Fig. 10. Visual grouping of coded sections within the six clusters shown in Fig. 8 into subclusters. Position of points determined by using the third principal-components (Z coordinates). Points not circled cannot be placed in any subcluster (see question marks in Fig. 9c).

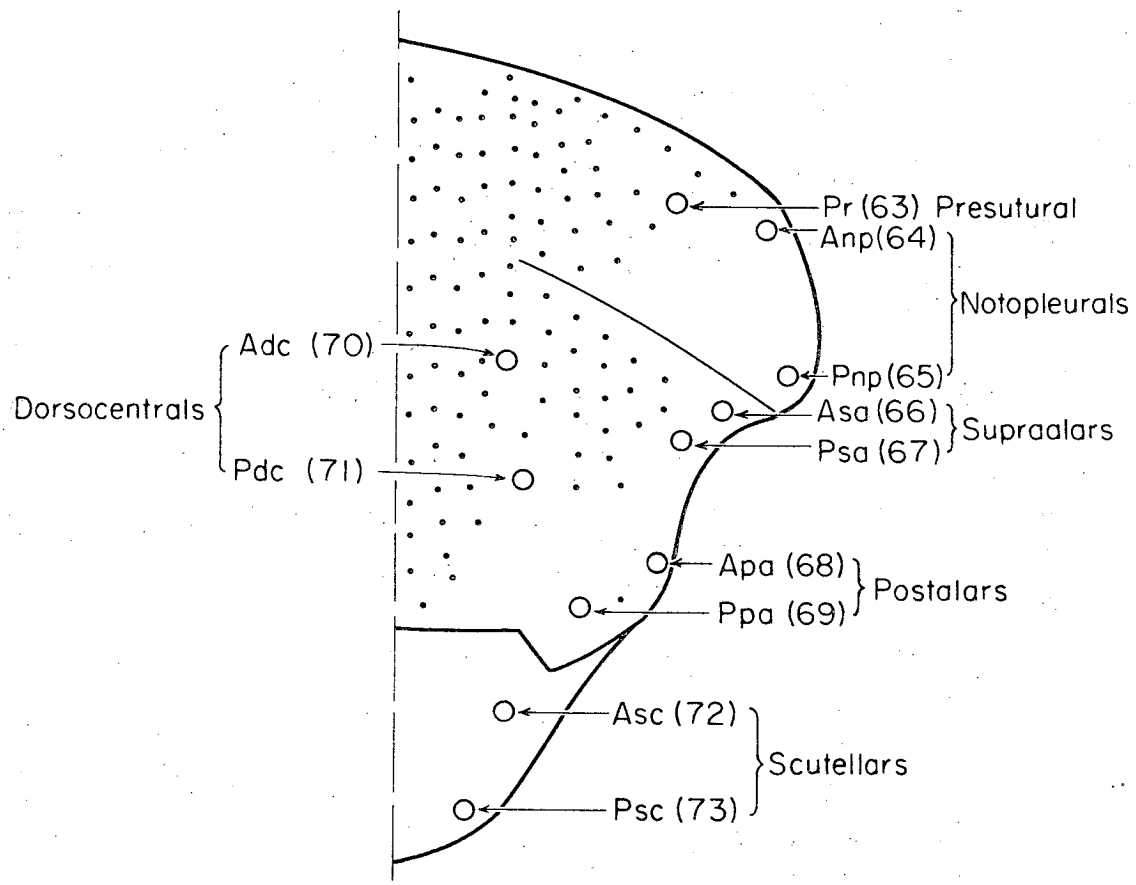

XBL 697-879

Fig. 1

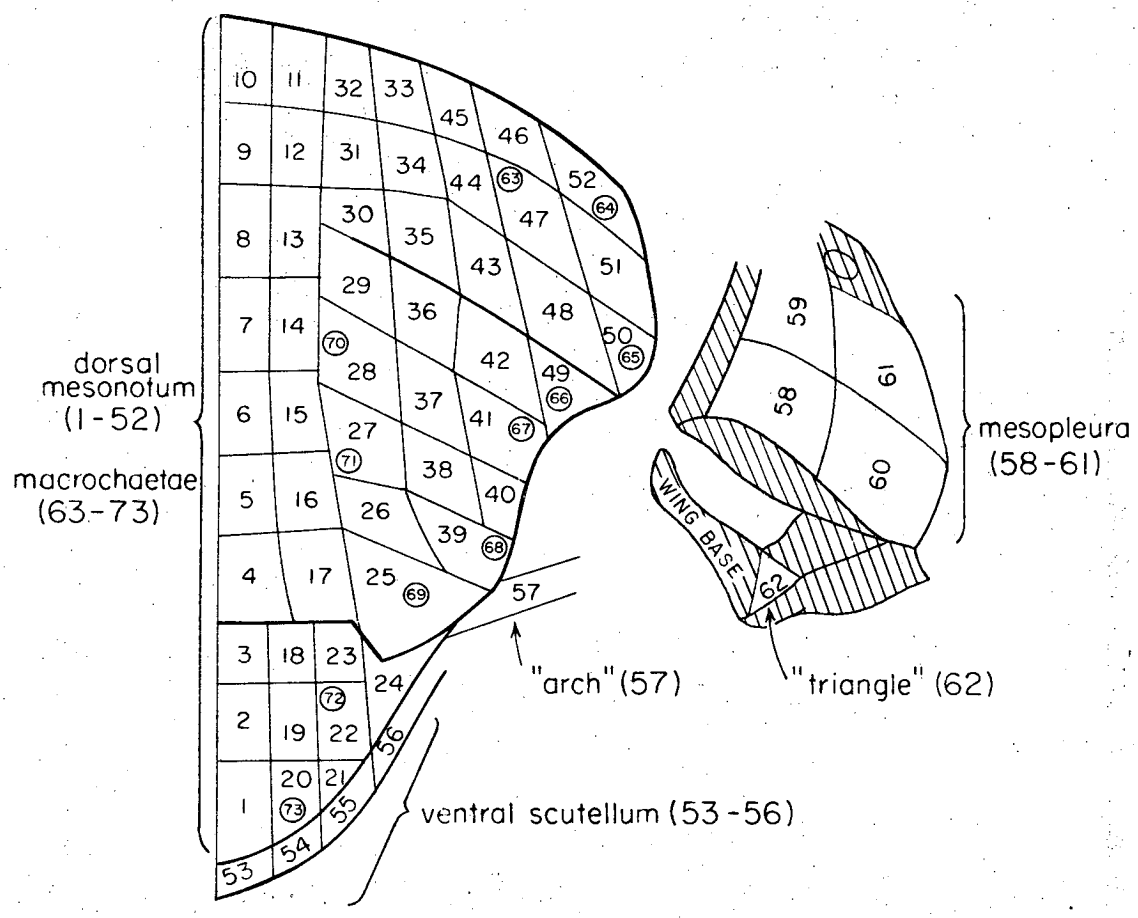

XBL 697-880

Fig. 2

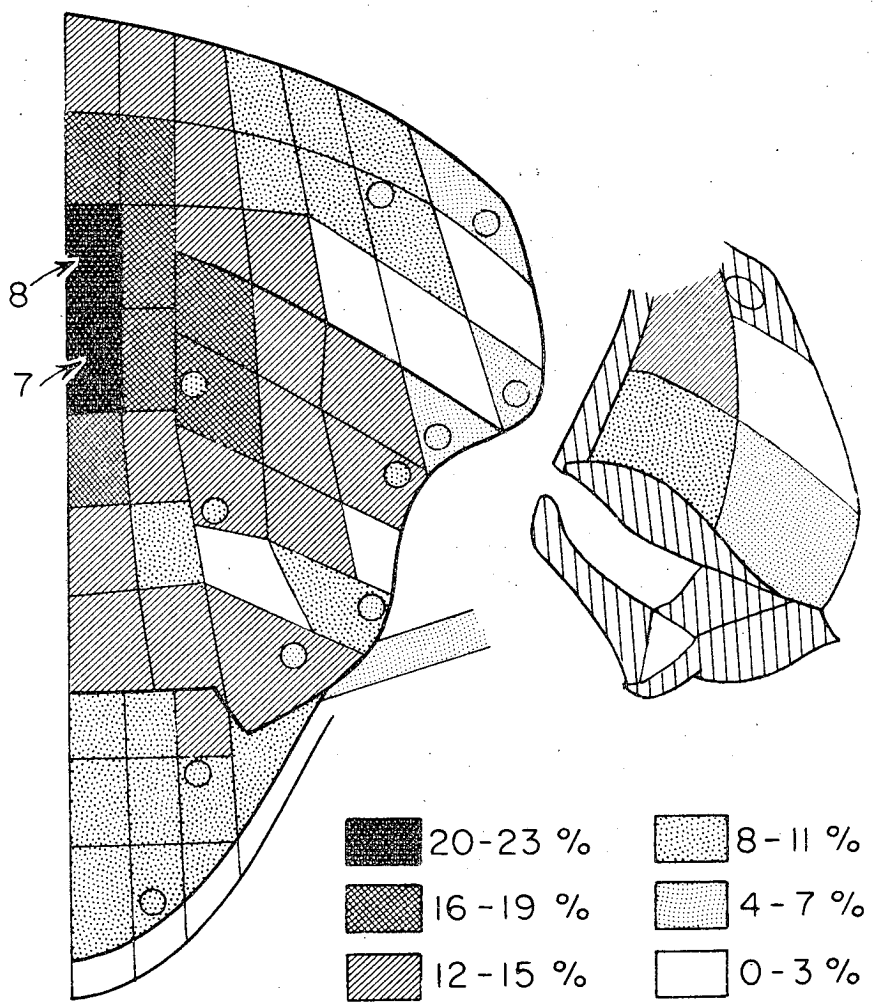

XBL 697-881

Fig. 3

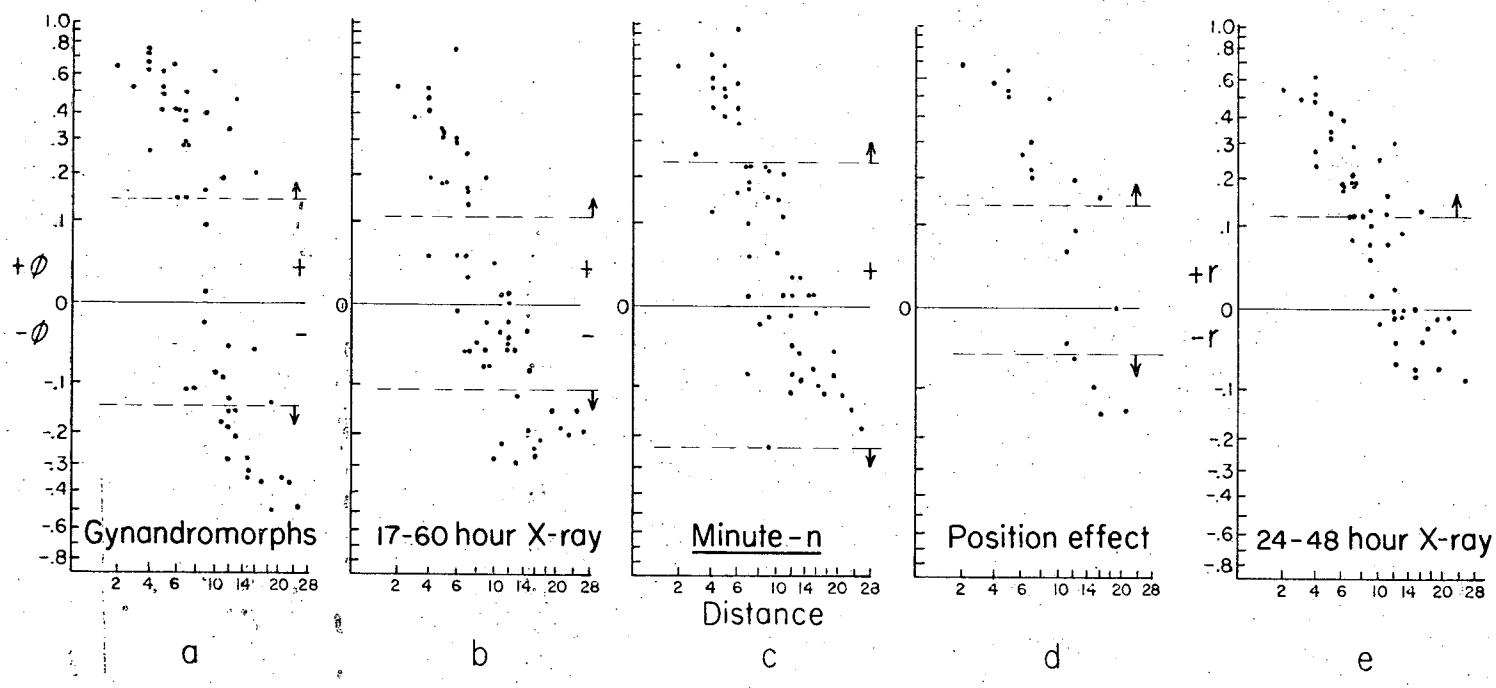

XBL 697-882

Fig. 4

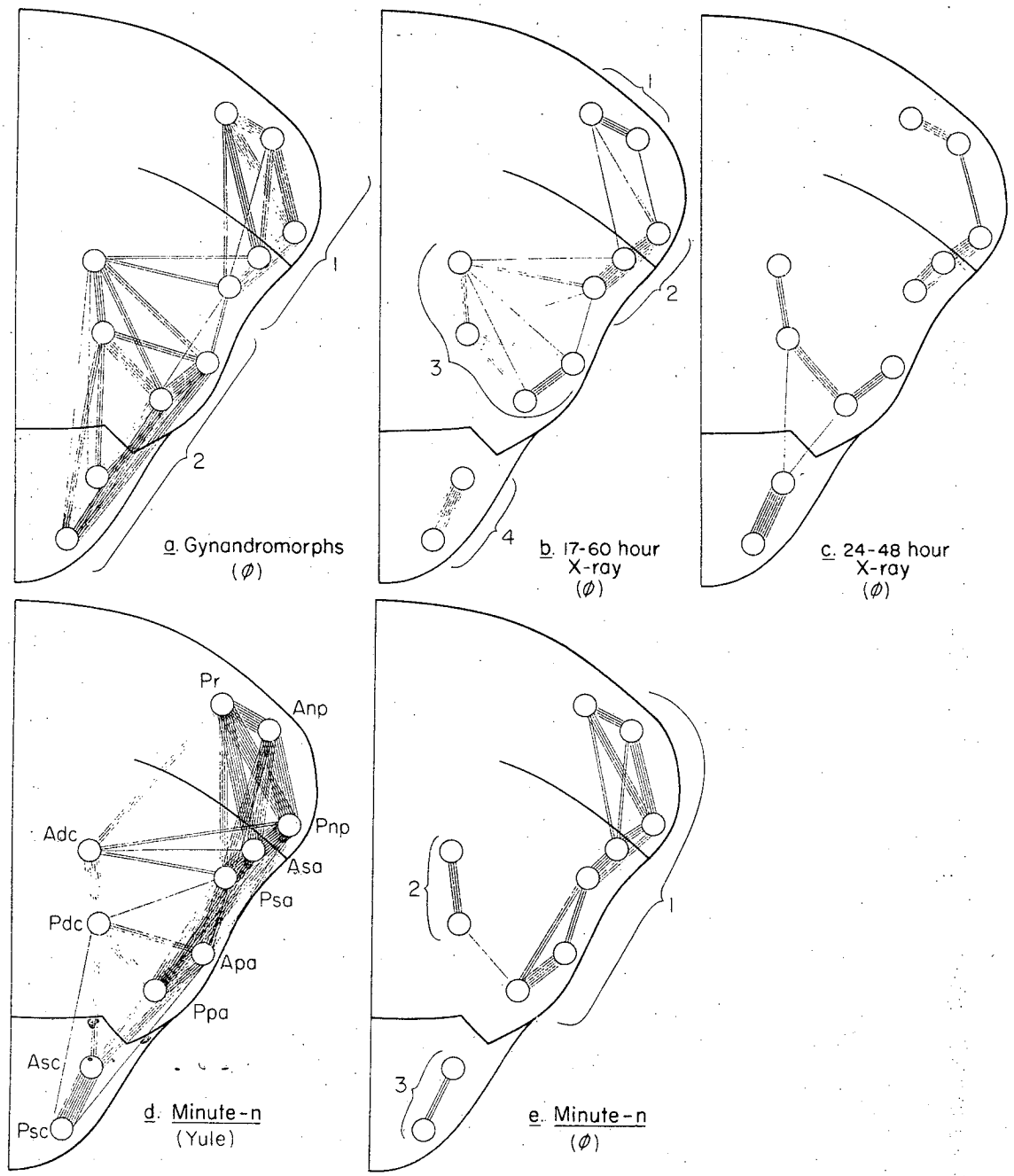

XBL 697-883

Fig. 5

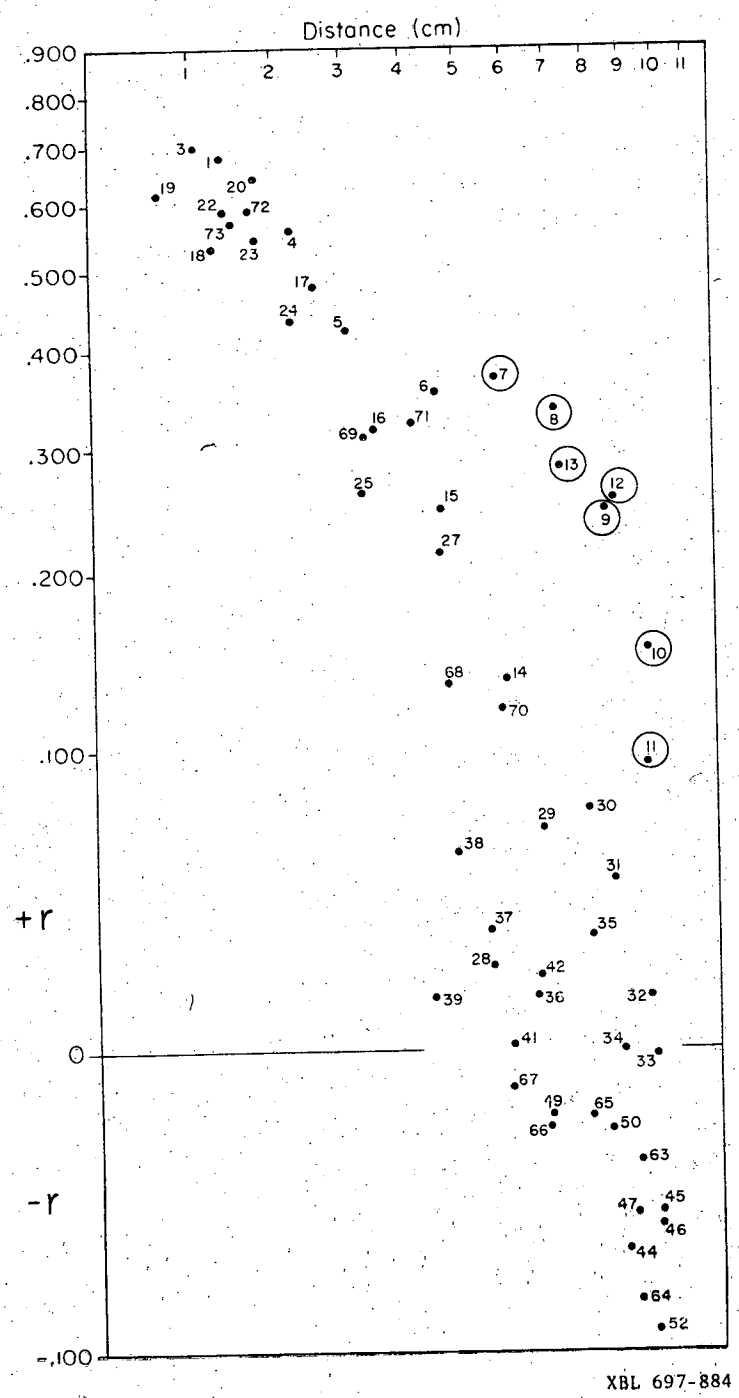
Distance (cm)
1
2
3
4
5
6
7
8
9
10
11
.900
.800
.700
.600
.500
.400
.300
.200
.100
0
-.100
+r
-r
XBL 697-884

Fig. 6

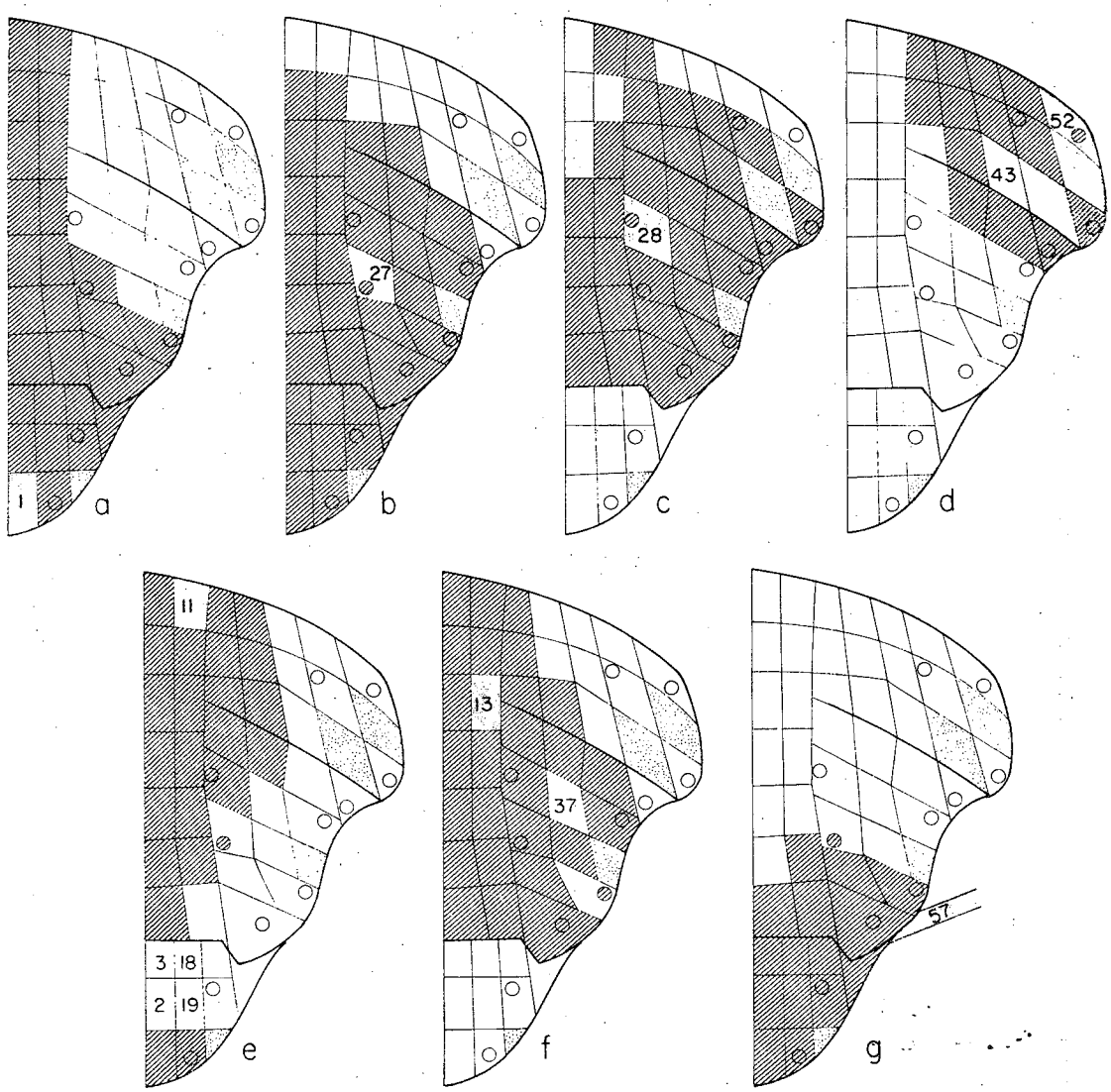

XBL 697-885

Fig. 7

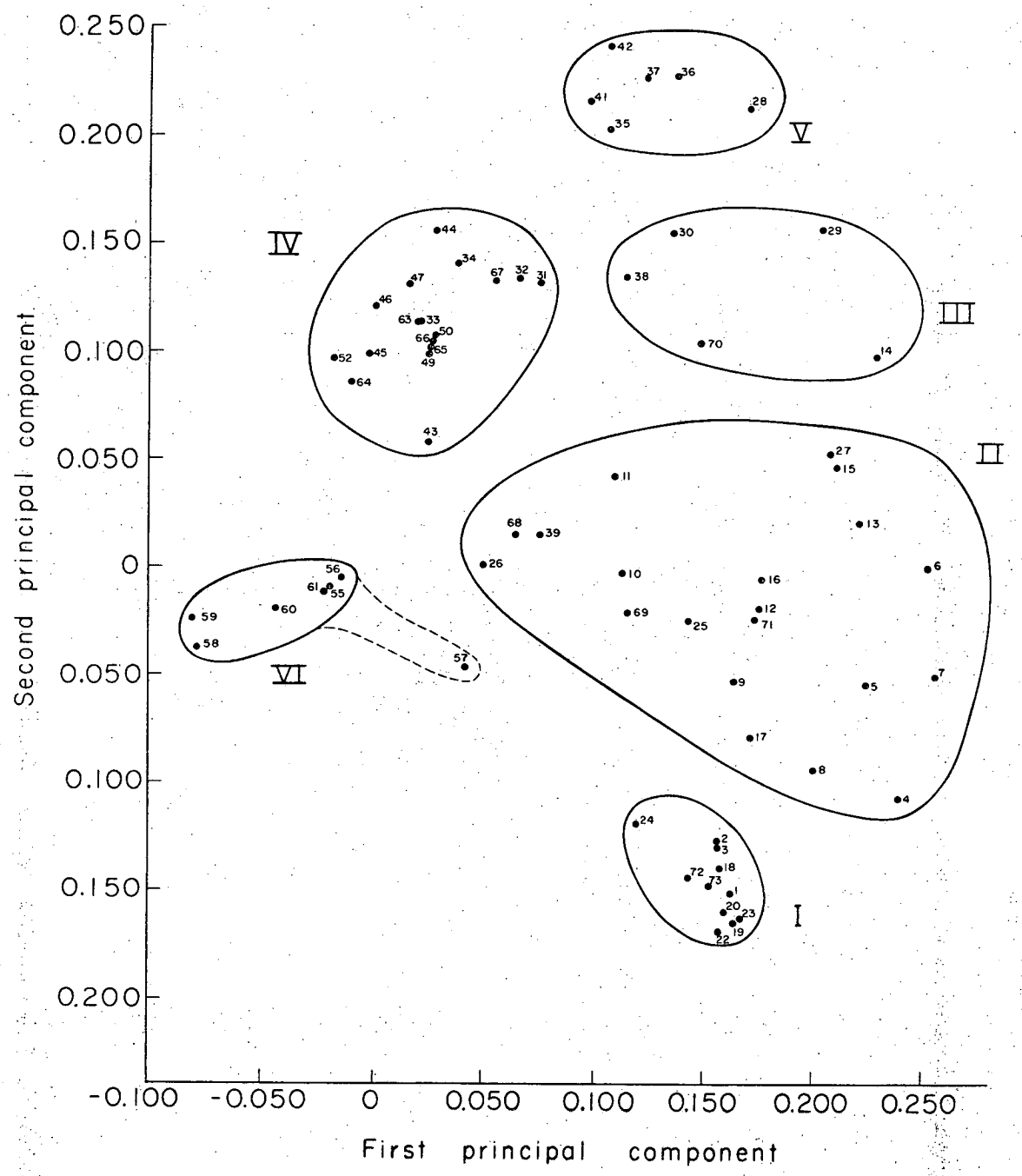

XBL698-3574

Fig. 8

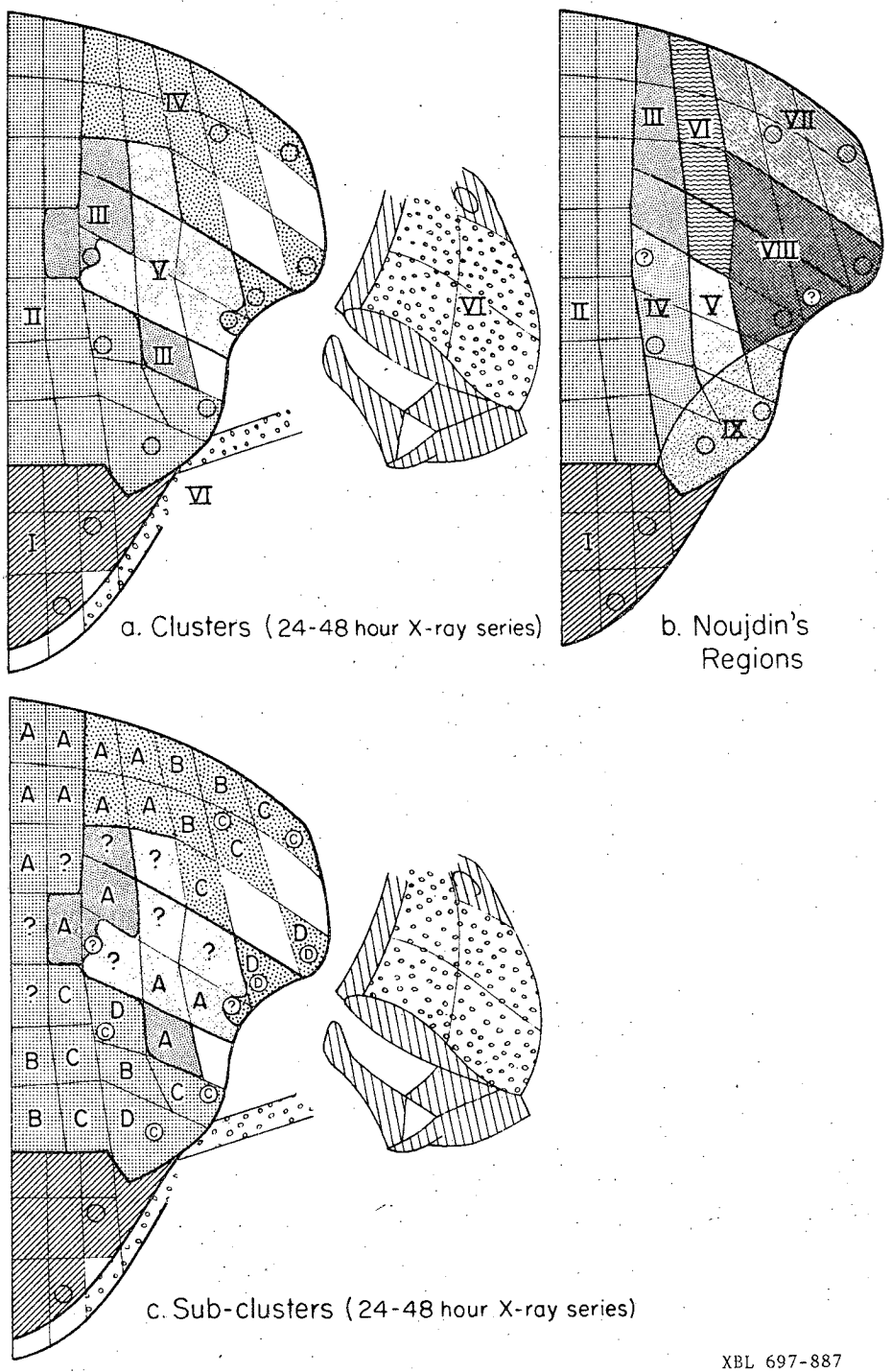

XBL 697-887

Fig. 9

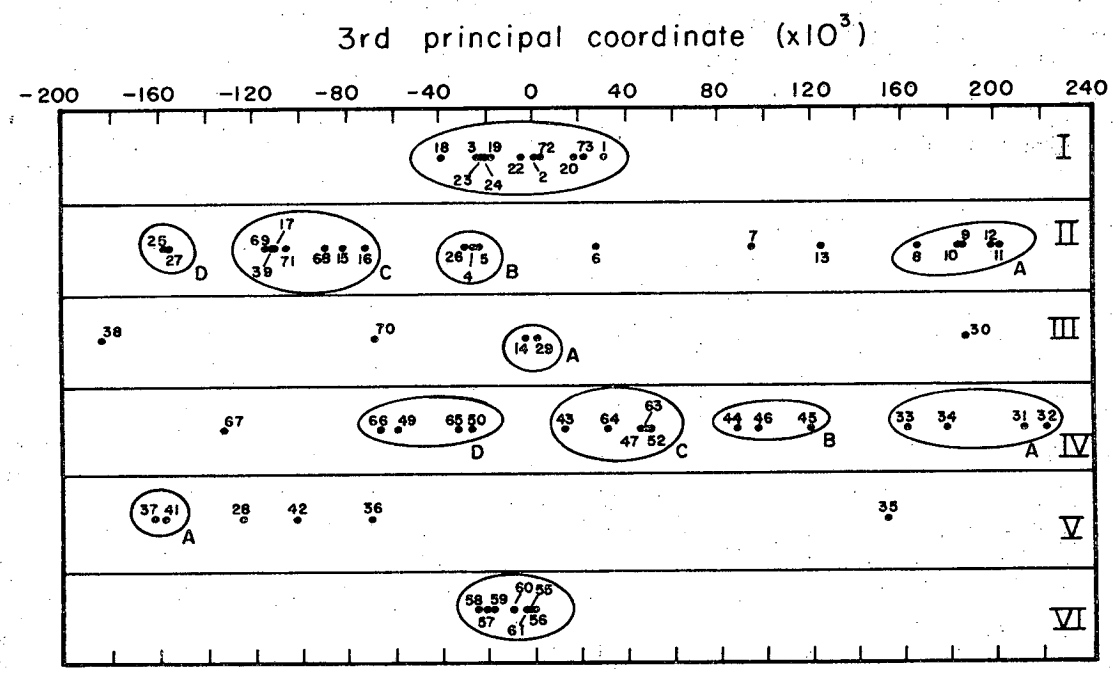

XBL699-3667

Fig. 10

LEGAL NOTICE

This report was prepared as an account of Government sponsored work. Neither the United States, nor the Commission, nor any person acting on behalf of the Commission:

A. Makes any warranty or representation, expressed or implied, with respect to the accuracy, completeness, or usefulness of the information contained in this report, or that the use of any information, apparatus, method, or process disclosed in this report may not infringe privately owned rights; or

B. Assumes any liabilities with respect to the use of, or for damages resulting from the use of any information, apparatus, method, or process disclosed in this report.

As used in the above, "person acting on behalf of the Commission" includes any employee or contractor of the Commission, or employee of such contractor, to the extent that such employee or contractor of the Commission, or employee of such contractor prepares, disseminates, or provides access to, any information pursuant to his employment or contract with the Commission, or his employment with such contractor.

TECHNICAL INFORMATION DIVISION
LAWRENCE RADIATION LABORATORY
UNIVERSITY OF CALIFORNIA
BERKELEY, CALIFORNIA 94720